January 2015

Design of a Surgical Manipulator System for Lumbar Discectomy Procedures

Benjamin V. Johnson
Purdue University

Follow this and additional works at: https://docs.lib.purdue.edu/open_access_theses

PURDUE UNIVERSITY
GRADUATE SCHOOL
Thesis/Dissertation Acceptance

This is to certify that the thesis/dissertation prepared

By Benjamin V. Johnson

Entitled
Design of a Surgical Manipulator System for Lumbar Discectomy Procedures

For the degree of   Master of Science in Mechanical Engineering

Is approved by the final examining committee:

David J. Cappelleri
Chair

Raymond J. Cipra

Rebecca Kramer

To the best of my knowledge and as understood by the student in the Thesis/Dissertation Agreement, Publication Delay, and Certification Disclaimer (Graduate School Form 32), this thesis/dissertation adheres to the provisions of Purdue University's "Policy of Integrity in Research" and the use of copyright material.

Approved by Major Professor(s): David J. Cappelleri

Approved by: Anil K. Bajaj   12/7/2015

Head of the Departmental Graduate Program   Date

DESIGN OF A SURGICAL MANIPULATOR SYSTEM

FOR LUMBAR DISCECTOMY PROCEDURES

A Thesis

Submitted to the Faculty

of

Purdue University

by

Benjamin V. Johnson

In Partial Fulfillment of the

Requirements for the Degree

of

Master of Science in Mechanical Engineering

December 2015

Purdue University

West Lafayette, Indiana

ACKNOWLEDGMENTS

I would like to express my sincere gratitude to Prof. David J. Cappelleri for his continuous support, guidance, patience and for providing the resources and environment for the course of this work. I would like to thank Dr. Brian Cole for his feedback from a surgeon's perspective which was key to the development of this work.

I would like to thank Prof. Thomas Siegmund and Yinglong Chen for providing the 3D printing facilities and support, without which this project would have been difficult to materialize. I would like to thank Prof. Rebecca Kramer for being a part of my thesis committee and for the material test facilities for the characterization of the materials used for this work. I would like to thank Michelle Yeun for her expertise and help for the use of the instruments in the lab.

I would like to thank Prof. Raymond J. Cipra who was always available to listen and share advice on many aspects of my project, and for being a part of my thesis advisory committee. I would also like to thank him for being patient with me during times when he was the course instructor for my teaching assistantship duties.

I would like to thank the School of Mechanical Engineering for the financial support through teaching assistantships during the course of my this work here. Special thanks to the donors of Harnek and Malkit Gill Scholarship Award that gave me additional financial support.

I would like to thank my lab mates who helped me through research discussions and valuable suggestions that helped me shape my project. I would like to especially thank Dr. Sagar Chowdhury for his insightful comments and constructive criticisms that helped shape this work.

Finally I would like to thank my parents and my brother for their constant encouragement and prayers, and for teaching me that 'I can do all things through Christ who gives me strength'.

TABLE OF CONTENTS

LIST OF TABLES

LIST OF FIGURES

ABSTRACT

Johnson, Benjamin V. MSME, Purdue University, December 2015. Design of a Surgical Manipulator System for Lumbar Discectomy Procedures.   Major Professor: David J. Cappelleri, School of Mechanical Engineering.

A 3D printed surgical master-slave manipulator system for minimally invasive lumbar discectomy procedure is proposed. Discectomy is the surgery to remove the herniated disc material that is pressing on a nerve root or spinal cord. This surgery is performed to relieve pain or numbness caused by the pressure on the nerve. The workspace is limited ($< 27\ cm^3$) and the manipulator has to go through a 3.175 mm (0.125") diameter channel. The proposed system is comprised of a family of manipulators that can work alone or co-operatively to perform tasks required in the surgery. In the proposed system, the manipulator is 3D printed with multiple materials, with flexible links acting as joints of the mechanism. These flexible links are actuated by cables which provide sufficient forces for actuation in the surgical workspace. In this thesis, existing surgical techniques are investigated and a new surgical system is proposed. Various design ideas are presented and evaluated for manufacturing and assembly. Finally, the proposed mechanisms are modeled and tested for their capability to assist the surgeon to perform tasks required for the surgery.

1. INTRODUCTION

The advancements in the field of surgery has lead to better healthcare and quality of living. New technologies implemented into surgical procedures have improved the success of the surgeries and added convenience to the patients. The foray of endoscopes and stereo vision has helped surgeons work through smaller incisions that have reduced discomfort, risk of infection and healing time for the patient. Such surgeries are called laparoscopic surgery, or Minimally Invasive Surgery(MIS). But this has not made the work of the surgeon any easier.

The demand for skilled surgeons have increased due to complications working under constrained spaces and limited dexterity. They often have to readjust postures which is often tiring. The repeated adjustments to the trocar also increases the risk of damage to the tissues. In smaller incisions, the surgeon has limited control of the workspace because of limitations related to number of instruments he can use.

Robotic interventions in surgery have improved many of these concerns involving the surgeon. Surgeons can work in an ergonomical environment, get a stereo view of the surgical workspace and use dexterous manipulators to operate the surgical workspace. But these systems are expensive, takes up space in the operating room and are not build for all types of surgical procedures. Also, difficulties in sterilizing such complex instruments and the life associated with these instruments raise costs. Also, the patient is affected by the high cost of such surgeries.

3D printing technologies have been pivotal in providing a cheap alternative for prototyping and evaluation of designs. Commercial 3D printers have the ability to create parts with complex geometries, which can be used with minimal assembly and actuation setup. The ability to create parts with multiple materials help in simplifying a variety of aspects of the design. With high resolution and accuracy, complex

geometries that would otherwise require expensive machining, can be designed and printed in a matter of minutes in such printers.

There is a need for a change in the way surgical instruments are made and used. Surgical systems should be designed for specific surgeries, and should ideally not take up a lot of space. By using modern manufacturing techniques, it is possible to reduce costs and create accurate complex parts easily that can be used without complicated assembly. The main objective here would be to not compromise on the quality of the surgery. This thesis proposes such a system for robotic surgery, for the specific case of lumbar discectomy surgery.

Hence there is a call for new instruments that are easier to use and cheaper to manufacture, without compromising on the quality of the surgery. The robotic system should provide the surgeon with ergonomical joystick controls of the instrument, and the ability to use multiple instruments at a time. This report proposes such a new system for robotic surgery, for the specific case of lumbar discectomy surgery.

In Chapter 2, existing tools used in surgery, and the lumbar discectomy surgery and techniques, are discussed. A new surgical system is proposed, and various design requirements are discussed in Chapter 3. Chapter 4 deals with the design of the end-effectors required for the surgery. In chapter 5, the designed end-effector prototypes are fabricated and evaluated for manufacturing. In chapter 6, the capability of the final designs of end-effectors for the surgery are measured for the requirements of the surgery, and the end-effector kinematic models are proposed. To conclude, in chapter 7, an overview of the proposed system is presented, and the results and future work are discussed.

2. BACKGROUND AND RELATED WORK

2.1 Robotic Systems for Surgery

Over the years, many devices have been created for assisting surgeons with surgery. They are designed to assist the surgeon to carry out various tasks during surgery that may include preoperative planning, intraoperative registration to presurgical plans, use of robotic assist and manually controlled tools to carry out the plan, and postoperative verification and follow-up [36]. Taylor and Staoianovici [36] have divided surgical robots into two broad categories, *surgical computer-aided design/manufacturing system (CAD/CAM) systems* and *surgical assistants.* Surgical CAD/CAM systems are designed to assist in planning and intraoperative navigation through use of images and three-dimensional (3D) models, allowing accurate execution of the planned interventions. Surgical assistants are divided into two classes: *surgical extendors*, which are operated directly by the surgeon and *auxillary surgical supports*, which work side-by-side with the surgeon and provide support functions, such as holding an endoscope.

Figure 2.1. Intuitive surgical da Vinci Surgical System [18].

The use of robotic assistant systems for surgery has risen rapidly in the few years. One of the most popular of these systems, Intuitive Surgical's da Vinci system (Fig.2.1), was used in 80% of radical prostatectomies performed in the US for 2008,

just nine years after it went on the market [2]. Through robotic assistants, surgeons are now able to access the surgical workspace with small incisions and still be able to operate with dexterity comparable with traditional operative procedures. Surgical assistants also offer intraoperative planning features to position and guide tools. Examples of such devices include neurosurgery robots such as the NeuroMate (by Renaissance, Integrated Surgical Systems) and Renaissance System (Mazor Robotics); and orthopedic robotic assistant devices like RIO (MAKO Surgical Corp.) and Robodoc (THINK Surgical Inc.). Robodoc utilizes the tandem technologies of TPLAN, a 3D planning workstation for preoperative planning and TCAT, a computer assisted tool that executes the pre-surgical plan.

Surgical assistants for general laparoscopy was first done in 1988 to remove soft tissues during transurethral resection of the prostate. Commercial robotic systems like Zeus (Computer Motion; and later licensed to Intuitive Surgical) and the da Vinci System (Intuitive Surgical) offered surgeons a teleoperated system with a variety of articulated instruments to operate the surgical workspace. Also, care was given to improve the surgeon ergonomics through introduction of a surgeon workstation with enhanced 3D vision of the workspace and joysticks with haptic feedback and motion scaling. The da Vinci system obtained the license for general laparoscopy and for several other procedures like thoracic surgery [4] and laparoscopic prostalectomy [32]. General laparoscopic techniques require multiple incisions in the body and are practiced in large operating workspaces.

Attempts to reduce the trauma of multiple incisions in the patient led to the developement of single incision Single-Port Access (SPA), LaparoEndoscopic Single-Site Surgery (LESS) and Natural Orifice for Translumenal Endoscopic Surgery (NOTES). The idea is to have a single incision or use natural orifices of the body to insert multiple instruments to access the surgical workspace. Examples of such devices include the EndoSAMURAI (Olympus Corp., Tokyo, Japan, and the Direct Drive Endoscopic System (DDES; Boston Scientific, Natick, MA)(Fig.2.2) [33]. These devices are flexible to pass through lumenal tracts to perform surgical tasks. But they suffer from

severe friction effects due to long trasmission channels which results in delayed instrument response. Several changes were proposed to combat these challenges; which includes the development the nebraska miniature robot. The long transmission channels were eliminated by actuating the joints directly. Although the design eliminated the challenges, there was an increase in size of the robot and the initial tests reported mechanical failure [45].

Figure 2.2.   Devices for NOTES surgery: Boston Scietific DDES (Left) and Olympus Corp. EndoSAMURAI (Right) [33].

Some medical robots under development include the RAVEN II and MiroSurge. The RAVEN II system (Applied Dexterity, Fig.2.3) is a research surgical robot distributed across universities all over the world. The MiroSurge system (Fig.2.4) was developed at the German Aerospace Center (DLR). It consists of 3 surgical robots (MIRO), out of which two carry instruments with force and torque sensors and one carry the stereo video laparoscope.

Robotic end-effectors for such procedures require to be dexterous, safe and provide sufficient forces for manipulation. Designs for such manipulators vary from being directly actuated rigid links, tendon driven rigid links, and continuum manipulators.

Directly actuated rigid links use mechanical linkages that extend from the base of the manipulator to the tip. The series of linkages transmit the forces to the end-effector. Multislider mechanism [43] and the link driven type multiple DOF forceps [34] are examples of such mechanisms (Fig.2.5). Recently, there have been few developments in the area which may be attributed to the required complexity
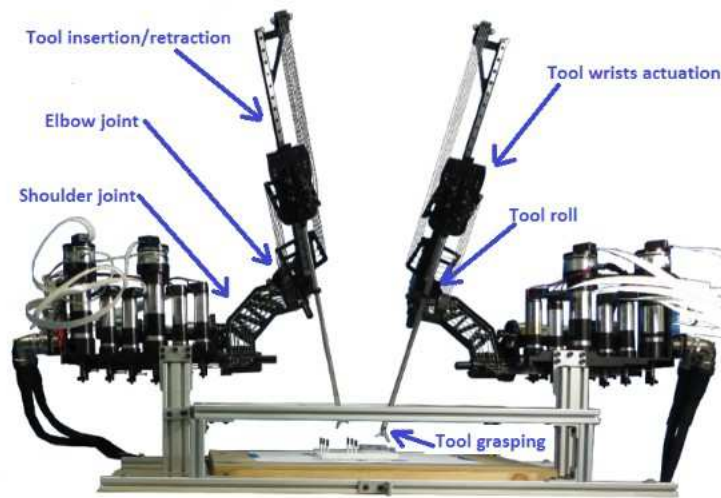
Figure 2.3. Raven II System [5].

of these mechanisms for sufficient articulation and difficulties in manufacturing and assembly.

Tendon or cable driven rigid robotic end-effectors for surgery has been popular due to their small size and the ability to use powerful actuators at the base of the robot. This is important to adapt to the developments in invasive surgical techniques which strive for smaller incisions. The commercially available EndoWrist instrument (Intuitive Surgical, Fig.2.6) is an example of such a device. The cables actuate the pulleys and joints at the tip for sufficient articulation which is able to mimic the movement of the wrist. Other examples include the MICA instrument(DLR, Fig.2.6) used by MiroSurge.

Continuum robots include robots shaped by continuously bending actuators, robots shaped by tendons, concentric tube continuum robots and steerable needles. These devices differ from the traditional surgical robots in rigidity and precision. But, these instruments are highly useful for their dexterity in highly clustered and unstructured environments [41]. Although there have been general models describing the behavior
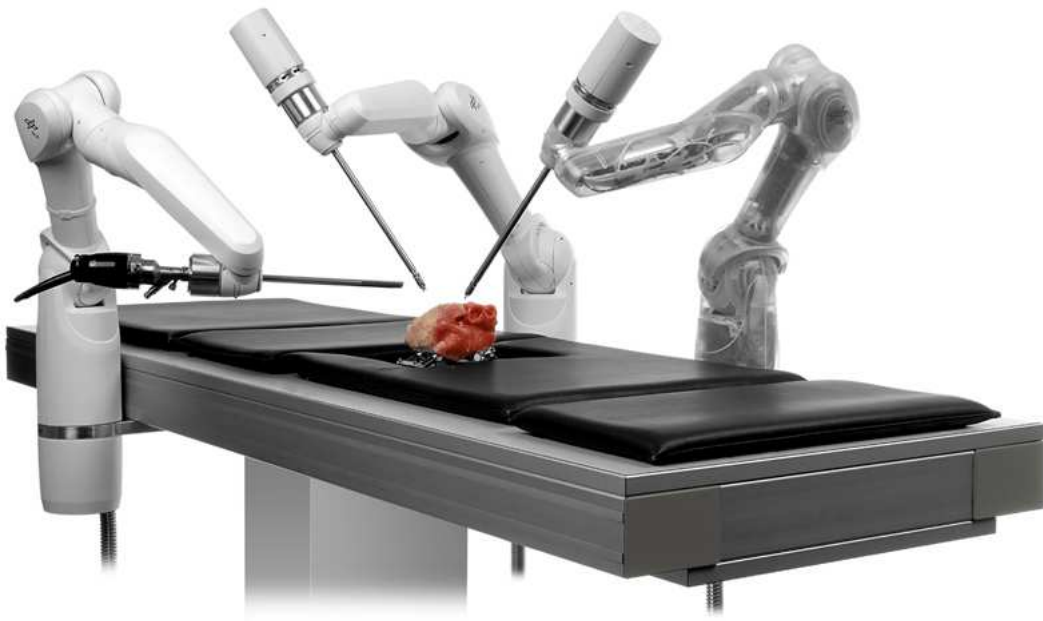
Figure 2.4. DLR MiroSurge Surgical System [8].
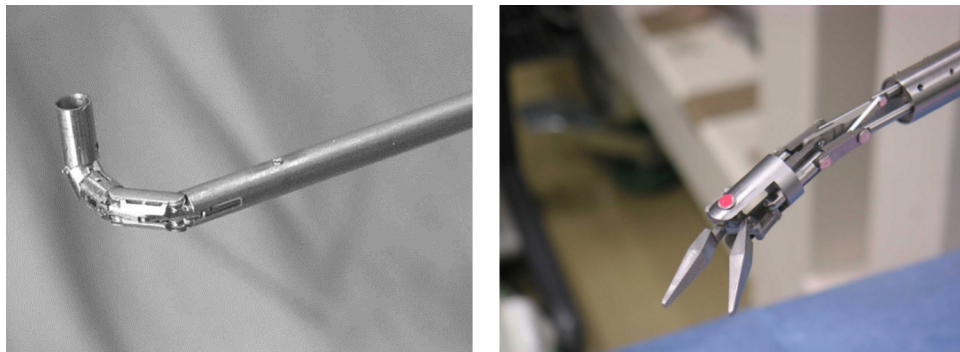
Figure 2.5. Multi-link mechanism based manipulators: 2-DOF minia-
ture manipulator based on multi-slider mechanism (Left) [44] and
Link driven multiple DOF forceps (Right) [34].

of continuum robots, considerable advances in this robotic theory is required for these
robots to fulfill its potential.

Figure 2.6.   Cable driven end-effectors: Link driven multiple DOF forceps (Left) [7] and Endowrist needle driver (Right) [17].

2.2   Systems for Spine Surgery

For spinal surgeries, issues like pedicle fracture, difficult visualization of the surgical area and high exposure of the patient, surgeon and clinical staff to ionizing radiation of the X-ray imaging which is used to guide the intervention, are common. Many robots were designed to tackle these issues in surgery. Over the years, robotic intervention in spine surgery [3] has focused on robots for screw insertion, laminectomy, and for needle-based interventions. Renaissance Guidance System (Mazor Robotics, Fig.2.7) is one such system which is used in pre-operative planning and implementation of spinal procedures through an accurate positioning system. It is important to note that several robots were also introduced for endoscopic interventions. These include MIcroNeuro-endOscopy of Spinal Cord (MINOSC) [1] , which is an endoscope designed to provide the surgeon with direct vision of the surrounding structures (spinal cord, blood vessels and nerve roots) through image processing techniques, and permits operations such as localized electro-stimulation by steering the endoscope tip to avoid obstacles. The da Vinci surgical robot (Intuitive Surgical, Sunnyvale, CA, USA), mostly used in urological and gynaecological surgeries, has also been tested for endoscopic spinal interventions. The practical applications here are limited because of their size and force capabilities. The existing tools are not

optimized for such surgeries, but there is reported use of prototype instruments for laminotomy, laminectomy, disc incision and dural-suturing procedures in [29].
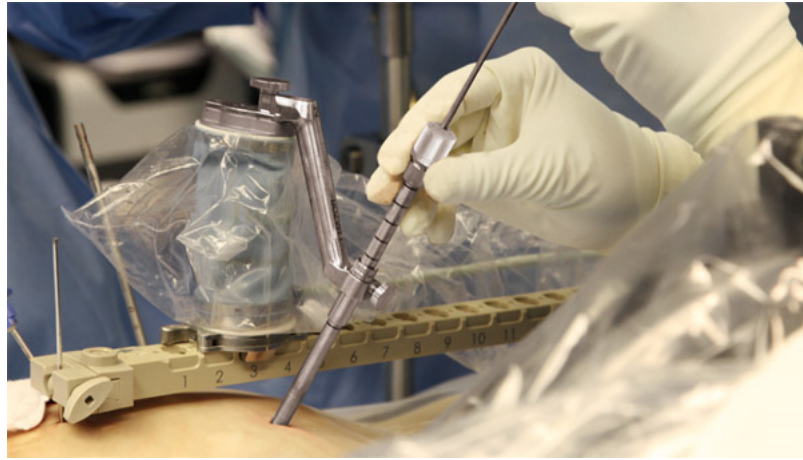
Figure 2.7. SpineAssist miniature device to direct surgical implants to spine [23].

Another area of spine surgery is the use of high-energy beams to ablate internal tumours. These radiosurgical systems employ heavy-duty robots that move a linear accelerator (LINAC) around the patient to fire the beams according to a predefined plan. This procedure is also used to ablate the herniated disk material [6]. Although this device performs well, it is not considered safe in conditions where the surgeons view is restricted, and hence it is not often preferred over traditional surgical techniques.

2.3   3D Printing in Medical Technology

3D printing or additive manufacturing techniques are mainly used as methods to create surgical implants for a variety of applications which includes skull, knee joint, elbow and hip joint. It is also used in the manufacturing of bridges and crowns in dentistry, and the manufacture of custom hearing aids. The ability to manufacture parts with complicated geometry, and the freedom to produce custom-build products give 3D printing based manufacturing techniques an upper hand in manu-

facturing implants. There are also several surgical tools developed for 3D printing. These include 3D printed retractor [30] and DragonFlex smart steerable laparoscopic instrument [19](Fig.2.8). The 3D printed retractor was manufactured in a Maker-bot 3D printer and the DragonFlex laparoscopic instrument was 3D printed using a ceramic-filled epoxy filled resin.
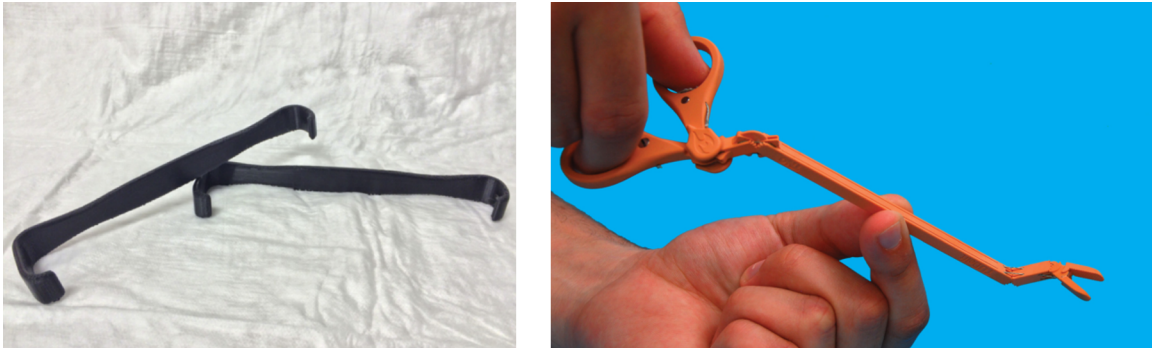
Figure 2.8. 3D Printing in Surgery: 3D printed retractor (Left) [30] and DragonFlex smart steerable laparoscopic instrument (Right) [19].

The 3D printed retractor was a successful attempt at recreating the existing retractors used for surgeries, and was able to replicate common Army/Navy instruments. The theoretical take on the merits of the implementation of 3D printing in producing cheaper alternative to the expensive steel instruments is pointed out in [19]. The DragonFlex instrument demonstrates the capability to have a feature-packed design based instrument, manufactured through 3D printing.

2.4 Existing Tools for Lumbar Discectomy Surgery

Currently, the only instruments available to remove herniated disc material consist of rigid probes with tips that manipulate and remove the patients tissue (Fig.2.9). These devices include, but are not limited to the Vertebris Lumbar-Thoracic Spinal Instrumentation, by Richard Wolf Medical, the fully disposable Mild, by Vertos Medical, and the Dekompressor, by Stryker. The use of these rigid probes (Fig. 2.9) is

much less efficient than using a robotic device because it forces the surgeon to re-adjust their position after every cut or maneuver. The inability to freely move within the restricted surgical workspace of the spine, which in some cases can be as minimal as a cubic centimeter, increases the risk of inadvertent damage of the spinal nerves, as well as other potential risks that can leave the patient paralyzed or requiring further surgery.

Figure 2.9. Rigid surgical instruments: Pituitary rongeur (Left) [16] and Penfield dissector (Right) [15].

2.5 Lumbar Discectomy Surgery

Lumbar discectomy surgery is performed to remove the herniated disk material that is irritating or inflaming the nerve root. The pressure on the nerve root can cause severe leg pain. In cases where conservative therapy is unsuccessful, such a surgery can provide immediate relief from the associated pain (Fig.2.10). There are various ways to perform this surgery. The traditional procedure is the open discectomy procedure. The most popular techniques include the micro-endoscopic discectomy and the athroscopic microdiscectomy.

2.5.1 Open Discectomy

Open discectomy is the traditional procedure to treat herniated lumbar discs. It was first described in 1934 by Mixter and Barr [31]. First, a skin incision, varying from 30mm to 60mm is performed, down to the subcutaneous tissue and the lum-
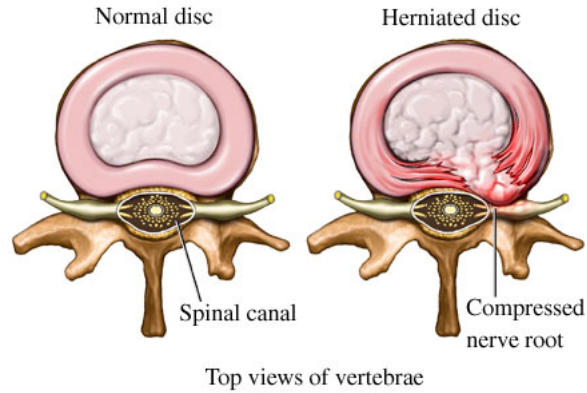
Figure 2.10. Herniated disc [27].

bodorsal fascia. A Williams self-retaining retractor is placed, and the muscles are swept laterally (Fig.2.11). A flavectomy and partial hemilaminectomy is performed to access the herniated disc. Epidural fat tissues and veins are dissected from the dorsal and lateral surface of the root, and bleeding veins are cauterized. The nerve root is retracted using a root retractor and the fragments of the herniated disc are removed using a pituitary rongeur. The herniated disc can also be incised using a microknife for the ease of removal. Once, the nerve root is decompressed, the retractor is removed and the wound closure is performed.

Open discectomy procedures require large incisions and causes severe trauma to the muscles and other soft tissues. This increases the healing time and discomfort, and hence might require extended hospital stay. Also, hemilamniectomy, the removal of a part of the vertebra is sometimes required.

2.5.2 Micro-Endoscopic Discectomy

Micro-Endoscopic lumbar Discectomy (MED) [26] is one of the most popular surgical techniques for lumbar discectomy. First, a 20-gauge (0.908 mm) spinal needle is inserted into the paraspinal musculature and repositioned using fluoroscopy techniques to place it over the disk space to be operated. The spinal needle is removed
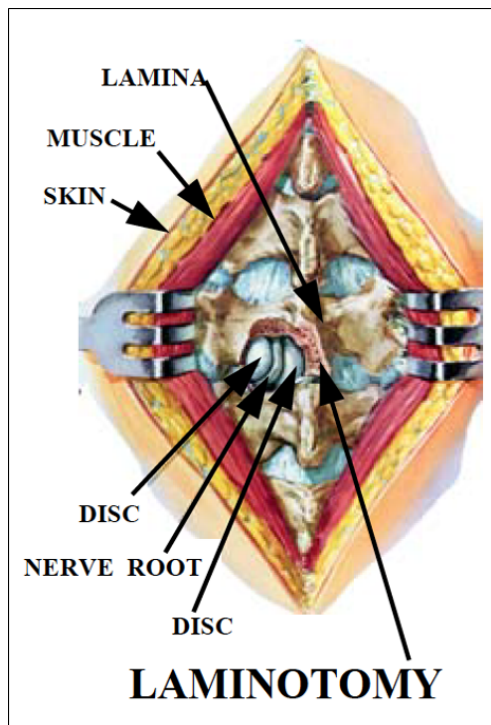
Figure 2.11. Open lumbar discectomy [10].

and an incision (around 24mm) is made to insert a tubular retractor. A guide wire is then placed through the incision and firmly docked into the bone. An dilator is inserted through the guide wire and a sequence of dilators are placed over it, which helps separate the muscles. Finally a working channel is placed over the final dilator (Fig. 2.12 A). The sequential dilators are removed to establish a tubular operative corridor to the lamina and interlaminar space. An endoscope is then inserted into the tubular retractor (Fig. 2.12 B) and fixed. A solution of plain saline is used as an irrigate to clear the camera during the procedure. The soft tissues over the lamina and interlaminar space are removed using a pituitary rongeur or a long tip insulated Bovie electrocautery tool. A hemilaminotomy, where a part of the lamina above and below the affected nerve is removed, is then performed using a high speed drill. The ligamentum flavum is then opened with an up-going angled curette. The nerve root can then be retracted medially using a penfield dissector to access the herniated disc.

The herniated disc material can then be removed using a pituitary rongeur. Once the nerve root is decompressed, the disc space is irrigated thoroughly before removing the surgical system assembly and covering the wounds.
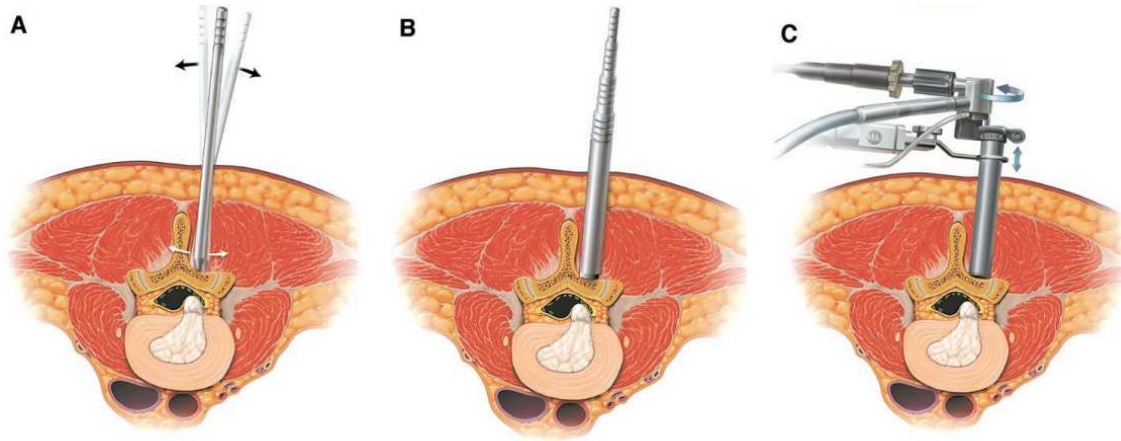
Figure 2.12. MED procedure steps: A: Dilator insertion, B: Tubular retractors, C: Retractor with endoscope [26].

MED is a huge improvement over the traditional open type surgery. Recent studies have shown that MED offers faster postoperative ambulation, milder postoperative pain, shorter hospital stay, shorter hospital delay and earlier return to work, compared to the standard lumbar discectomy procedure [22]. Although the procedure is effective, there is a learning curve for surgeons to use the system efficiently and safely. Surgeon comfort is often sacrificed as the surgeon has limited control of the position of the endoscope in the retractor and is forced to move the retractor around to find an optimal position to perform the surgery. This leads to further damage to muscles and soft tissues surrounding the retractor.

2.5.3 Arthroscopic Discectomy

Arthroscopic Microdiscectomy was introduced around the same time as MED [20]. This surgery can be performed through one or two ports by means of endoscope(s)

inserted through 1 cm skin incisions. Unlike MED, the protective bone and ligaments over the posterior surface of the vertebral canal are not broached. Hollow tubes (cannulas) approximately 0.25" in diameter are passed through the skin and muscle layers, through the right and left side of the patient, or both from the same side (Fig. 2.13). Using flouroscopy or an endoscope, the surgeon is able to position the cannula directly under the outer layer of the annulus and a wide (posterior longitudinal) ligament, which separates the disc from the contents of the spinal canal. The disc fragments can be removed using the pituitary rongeur (Fig. 2.9) with or without the help of the endoscope.
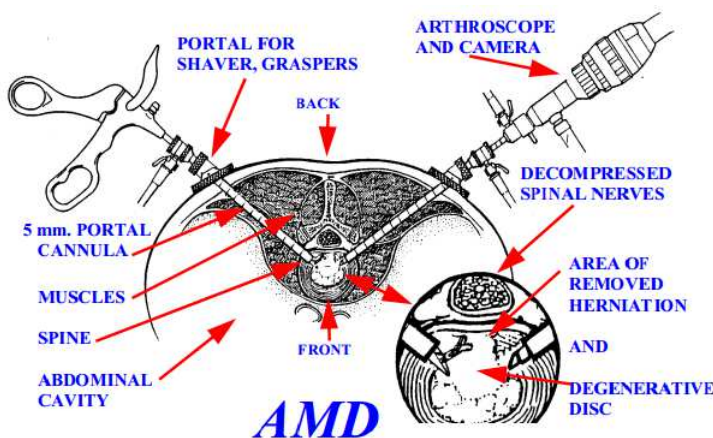
Figure 2.13. Arthroscopic microdiscectomy [42].

Arthroscopic Microdiscectomy has been successful compared to the traditional laminotomy and discectomy [12]. The patients who underwent arthroscopic microdiscectomy did not require overnight hospitilization, returned to work and resumed their activities sooner and required lesser postoperative pain medications and long-term narcotic use than patients that underwent the traditional open procedure. However, arthroscopic microdiscectomy requires a steep learning curve and requires a lot of patience and experience from the surgeon. The surgeon can be uncomfortable during the surgery as vision and dexterity in the workspace is extremely limited. The limited tools for the surgeon also forces him to operate blindly at times to access the

herniated disk material. As most of the tools are made of rigid materials, there is a chance of injury to the soft tissues or nerve root in the workspace.

2.6 Major Challenges

The major challenges for conducting the surgery is presented here.

2.6.1 Number of Tools

One aspect of the existing techniques is the limitations of the number of tools that the surgeon can operate in the workspace at the same time. In AMD, the surgeon is forced to use only one sub-3mm instrument at a time. These instruments are not articulated to reach the entire workspace and hence the surgeon needs to adjust the position of the cannula frequently to reach the desired point during the surgery. This also limits his ability to do multiple tasks simultaneously.

2.6.2 Surgeon Fatigue

Laparoscopic surgery tools have higher handle forces than conventional instruments because of their size/design limitations [11]. In AMD, there is no provision for the surgeon to position the instrument at the surgical workspace, for example, to retract the nerve away from the surgical workspace so that the disc herniation can be accessed. The surgeon is them forced to adjust the position of the cannula along with operating the tool which adds stress to the operating procedure. There is a trend of more shoulder stiffness after laparoscopic operations compared to traditional open surgeries [24].

2.6.3   View of Surgical Workspace

The view of the surgical workspace was good in the open procedure. But, with the smaller incisions and the restricted port sizes, the view is limited because of the absence of articulation for the camera. In case of AMD, the camera is adjusted by rotating the cannula which can further traumatize the tissues surrounding it, leading to longer healing time.

2.6.4   Surgeon Training

The drastic reduction in patient trauma from the surgery. It has also reduced blood loss during surgery and the shortened hospital stay after the surgery. But with the smaller incisions and the retricted workspace, the surgeons have to be cautious while navigating the surgical workspace due to the limited view of the operating area and the rigid tools that they are equipped with. At times, the surgeon is also forced to operate the workspace blind. This can potentially lead to dangerous situations where the nerve roots can get damaged. As a result, the surgeon requires long and extensive training to develop the required skill to operate safely. The availibility of these surgical instruments can also help in the training of surgeons, which in turn improves their skill and the chances of success for the surgery.

2.6.5   Sterilization

Sterilization of surgical instrument has reduced he risk of infections due to the presence of pathogenic microbes in an used instrument. It is not easy to sterilize surgical instruments, as it requires resource-rich settings to complete the sterilization guidelines. This includes the cost of the staff, maintenance of equipment, and unitilities, which increases the maintenance cost of the surgical system. As the complexity of the mechanism increases, it is difficult to sterilize it optimally.

2.7 Motivation

The rise of minimally invasive surgical techniques for lumbar discectomy has improved the patient recovery time, reduced blood loss during the surgery, and reduced hospital stay of the patient, thereby improving convenience and reducing costs for the patient. This has placed excess emphasis on the skill and experience of the surgeon. The reduced workspace has placed constraints on the surgeon and there hasn't been significant improvements in instrument design to combat these deficiencies. The idea of creating a new system of manipulators that give the surgeon the freedom that an open lumbar discectomy surgery offers, but can still pass through a incision, a size of a dime, is the objective of this project.

The challenges of the surgery are explored, and a surgical system is proposed. Tools for the surgical system are designed, prototyped, and tested to assist the surgeon for conducting lumbar discectomy surgery.

3. DESIGN OVERVIEW AND SYSTEM REQUIREMENTS

3.1 Proposed System Overview

In this section, a design outline of the system is described. The system mainly consists of the following components

1. Cannula

2. Manipulators

3. Actuator Box

4. Joystick

5. Endoscopic Camera System with Monitor

6. Irrigation System

The overall schematic of the system is shown in Fig.3.1

The patient will be awake during the surgery. This is to ensure that the surgeon is not exerting excessive pressure on the nerve roots in the surgical workspace. The patient would be lying on his stomach (Fig.3.2) and a procedure similar to AMD would be used to locate the workspace and position the cannula appropriately. This system can be mounted on a positioning robot or a fixture that is attached to the body of the patient or the surgical table.

The orientation of the cannula can be seen in Fig.3.3. There would be provision to insert multiple tools at a time. The tools are designed to work together in the workspace and there is the liberty of choosing the insertion port for the instrument, for the surgeon. The surgeon will control the manipulators using a set of joysticks that control the movement of the manipulator. The endoscopic camera system and

20
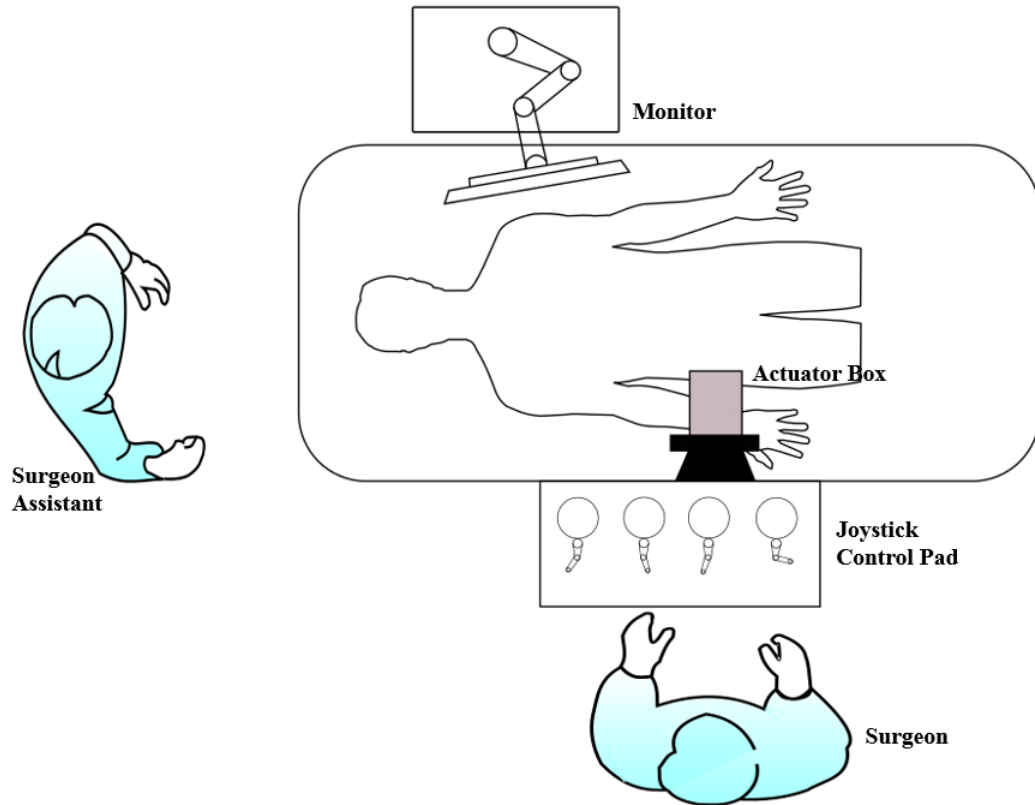
Figure 3.1.   Proposed system schematic.
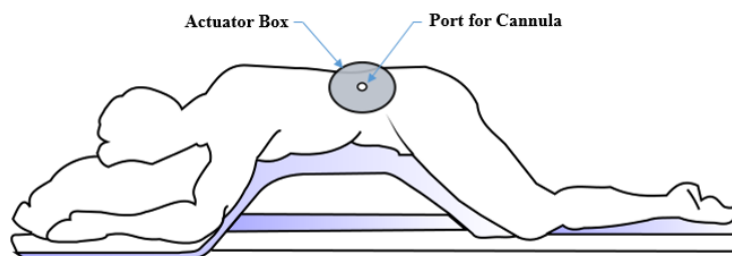
Figure 3.2.   Orientation of patient during surgery.

the irrigation system used to clear the workspace will also be designed to go through the same port which makes the system flexible.
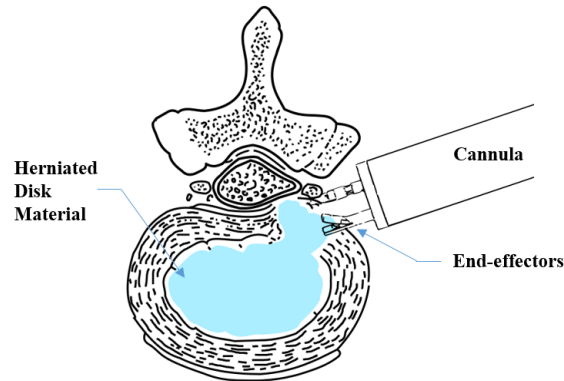
Figure 3.3. Surgical workspace schematic.

The actuator box would allow the surgeon to hold a manipulator at a particular position without actively controlling it. This enables the surgeon to use multiple instruments at a time. The actuator box would control all the manipulators, the endoscopic camera and the irrigation system, all the same way.

3.2   Design Requirements of the System

3.2.1   Cannula

The design of the manipulator system is defined by the restrictions of the various parts of the system. The most crucial of these is the cannula. The size of the cannula is restricted by the size of the incision. The target size of the cannula is in the range of 15-20 mm (diameter), which is the range for such surgeries, less than that of MED. Since there is a need to use multiple tools at the same time, there should be provision for multiple tools to access the workspace at the same time. Apart from the tools, there should be ports for endoscopic camera, lighting, irrigation and suction systems.

To improve the flexibility of the system, all the ports are designed to be the same size. The tools, camera, lighting, irrigation and suction systems should be designed to be inserted through these ports. This also ensures that the traditional tools that are usually $< 3.175mm$ (0.125") in diameter, can be used in cases of emergency.

Cannula Design: The cannula, or the instrument cannula should be able to support multiple tools and also be smaller in cross section compared to open discectomy or MED. Hence, the diameter of the cannula was chosen to be 190 mm. A proposed cross section of the cannula is shown in Fig. 3.4.
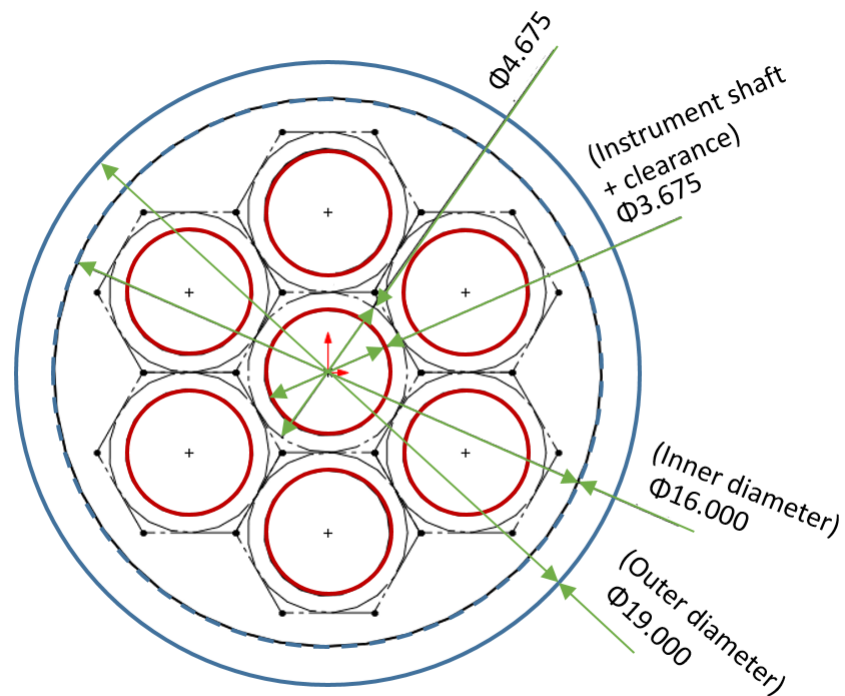
Figure 3.4. Cannula schematic.

The target port size for the instruments is chosen as 3.675 mm, which allows the passage of tools designed with 3.175 mm (0.125") diameter constraints, and the existing tools used in the surgery, in the event of an emergency. There is a provision of inserting seven instruments at a time. All these instruments would be designed

with the same diameter constraint and hence would be able to adjust the position of the tool based on the circumstances.

The length of the cannula would be in the range of 150-300 mm based on the patient. To enable easy sterilization of this device, the cannula was designed to be composed of a regular shaft with two adapters at each end with the required cross sectional features to allow for the insertion of instruments (Fig.3.5).
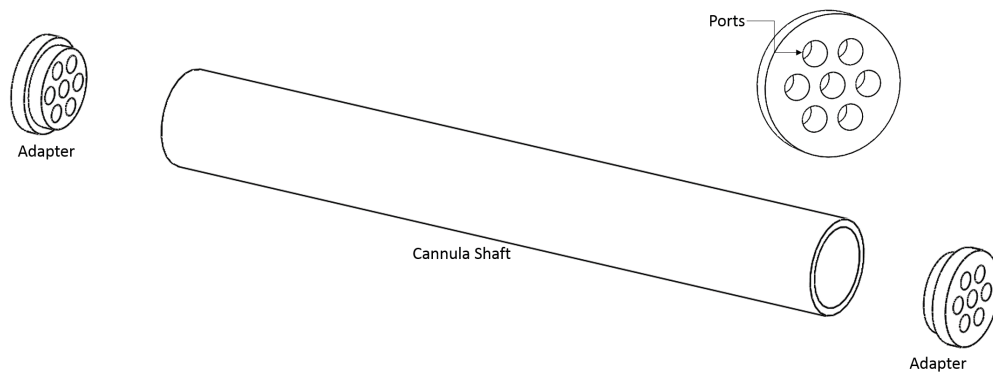
Figure 3.5. Cannula shaft and adapters : Exploded view.

3.2.2 Instrument Shaft

The end-effectors can be positioned at the operating space using 3.175 mm (0.125") diameter tube, which is called the instrument shaft. The complex end-effectors can be manufactured separately or along with the instrument shaft. The manipulator hence can be divided into the instrument shaft and the end-effector which can be connected to the shaft, that can be actuated in the workspace. It is important to design end-effectors that can improve or mimic the capabilities of the existing instruments. The cost of manufacturing should also be taken into consideration. In case

the tool cannot be sterilized, the manufacturing cost should be low enough for it to be disposable.

Instrument Shaft Design: The instrument shaft functions as the bearer of the end-effector to deliver it to the workspace. The shaft needs to carry the cables that will operate the end-effectors, and itself be actuated to improve the access of the end-effector in the workspace. To replicate the motions of the existing instruments, the shaft needs to have (Fig.3.6)

1. Ability to move along its axis (Translation)

2. Ability to rotate along its axis (Roll)

The translational ability will ensure that the essential functions like moving into the workspace or pulling the herniated disc material can be done. Also, the roll motion would improve the accessibility of the end-effectors in the workspace and provide twisting motion to the end-effector if necessary.
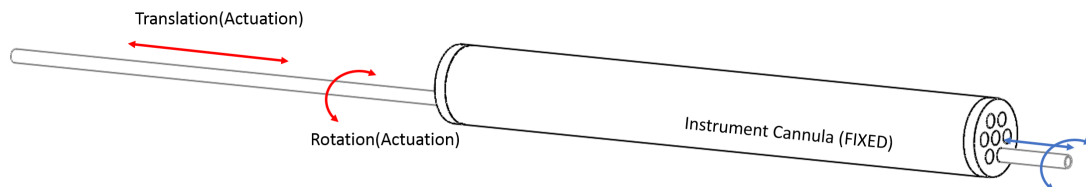
Figure 3.6. Instrument shaft schematic.

3.2.3 Endoscopic Camera System and Irrigation System

The endoscopic camera system requires to consist of the camera and the lighting system. They can be a combined unit or separate camera and lighting units. Each can fit into the 0.125" diameter port. The camera can also be the end-effector,

where a special port can be used to mount the camera to an existing multi-degree of freedom joint. This allows for changing the orientation of the camera if necessary. Similarly, multiple lighting sources can be used for the surgery, if needed. An example of endoscopic camera with lighting system that can be used, is shown in Fig.3.7. A saline irrigation system is used to clean the endoscopic lens of accumulated fog or blood. This system will also go through the port.

Figure 3.7. Medigus microScout camera (2 mm diameter) [21].

3.2.4   Joystick System

The surgeon should able to see the workspace shown by the endoscope through a monitor. He/she can control the system using a set of joysticks like a master-slave system. The joysticks would be able to gather movements for cooperative manipulation and tranfer it to the end-effectors. The system will also have features to lock on the position for a given end-effector, for example, to retract a nerve, so that the surgeon can handle the delicate movements of the other end-effectors efficiently.

3.3   End-Effector Design Requirements

The end-effectors should be designed keeping in mind the restrictions posed by the cannula (Sec.3.2.1) and the instrument shaft (Sec.3.2.2). But, it is very difficult to

design complex mechanisms, with pin joints, for a 0.125" diameter instrument shaft. Hence, it was decided to replace the required pin joints in the assembly to flexible members. These members can act as a pseudo joint and give the required function without the complexities of the traditional manufacturing techniques.

3.3.1 Nerve Retractor

The existing nerve retractors (Fig.3.8) have the ability to hold the nerve away from the disk herniation. The usual instrument has a hooked, or angled blade fitted at the end. This allows the surgeon to push the nerve root away from the surgical site during the operation. Since the end is rigid, the surgeon needs a large space to orient the tool to access the nerve root, especially in MED. In AMD, the surgeon adjusts the position of the cannula to move away from the nerve root to access the surgical space. This can be dangerous as the end of the cannula would be too close to the nerve.

Figure 3.8. Nerve retractor [14].

1. The main design objective of a new retractor was to allow sufficient articulation at the tip to retract the nerve so that the grasper could access the work space. The proposed designs were a 1 DOF or 2 DOF end-effector which can reach the area and move the nerve aside.

2. The actuation range for the retractor was chosen to be 80° $(-40°, +40°)$. This allows the instrument to enter the workspace through the port and retract the nerve away from the herniated disc material.

3. The literature for force requirements of lumbar discectomy surgery is non-existent. In laparoscopic procedures, the forces are in the range of 5-10 N, which are difficult to attain for miniature devices [38]. The force capabilities for the manipulator should be enough to perform the basic tasks during the surgery. The soft tissue manipulation force is about 0.45 N [38]. In cases where the nerve roots are involved, it was found that high forces of upto 0.4 N can lead to nerve damage [9]. More than 70% of forces applied during the neurosurgical tasks were less than 0.3 N, while the forces for dissection and coagulation ranged from 0.16 N to 0.65 N.

   The force required for the retraction should be more than the nerve root pressure. The nerve root pressure before discectomy varies from 7 mmHg to 256 mmHg (mean, 53 mmHg) [35]. Hence the joint should be able to exert pressures in the range from 0.000933 N/mm^2 to 0.0341 N/mm^2. Considering a surface area of 10 mm^2 for the end-effector, the maximum force required is 0.35 N.

   For grasping, the forces requirements are higher. The grasp action will also include the pull force required in during the operating. The pull force is regulated by the shaft pulling the grasper, which should be in the range of 5-10 N.

3.3.2 Grasper

The existing graspers used for pulling out the disk herniation are of two sizes. The 5 mm diameter tool has an articulated end along with the grasping mechanism. Due to its large size, this tool cannot be often used with an endoscope and hence the surgeon often has to operate the workspace blindly. The other tool that is used with an endoscope is the 3 mm diameter tool. This tool doesn't have any articulation at the end.

Other issues with such tools is the inability to use these tools simultaneously with the nerve retractor or any other tool. Also, these tools are difficult to position as the surgeon has to rely on the endoscope vision, orient the tool to position the tool and then use the grasper to pull out the herniation. This puts a lot of pressure on the surgeon as he is operating in a restricted environment.

1. Ideally, the grasper should have enough articulation at the end, for effective manipulation. The grasper jaw should also open wide enough to sufficiently grip the tissue that needs to be pulled out.

2. The grasp forces would be lower compared to traditional graspers used for surgery since we are dealing with soft tissues. There is a scarcity of literature regarding the specific forces required for grasping during lumbar discectomy surgery. A rough range of handle forces and tip forces were calculated across tissues of variety of stiffness. It was found that the grasp pinch force for soft tissues range to about 0.2 N [37]. The other force required is the pull force which is usually in the range of 5-10 N.

3. The traditional single jaw grasper has a jaw angle of about $30 - 45°$. The double opposing jaws have angles upto $90°$. This ensures sufficient grip during the grasp of the herniated disc material. The jaws are usually designed to be in open configuration when not actuated.

4. END-EFFECTOR MODELING AND DESIGN

4.1 Nerve Retractor

4.1.1 Mechanism Design

There are several ways to design a 1 DOF actuated end-effector. Flexible links are used here to replicate the function of pin joints. An example of such a mechanism is shown in Fig.4.1.
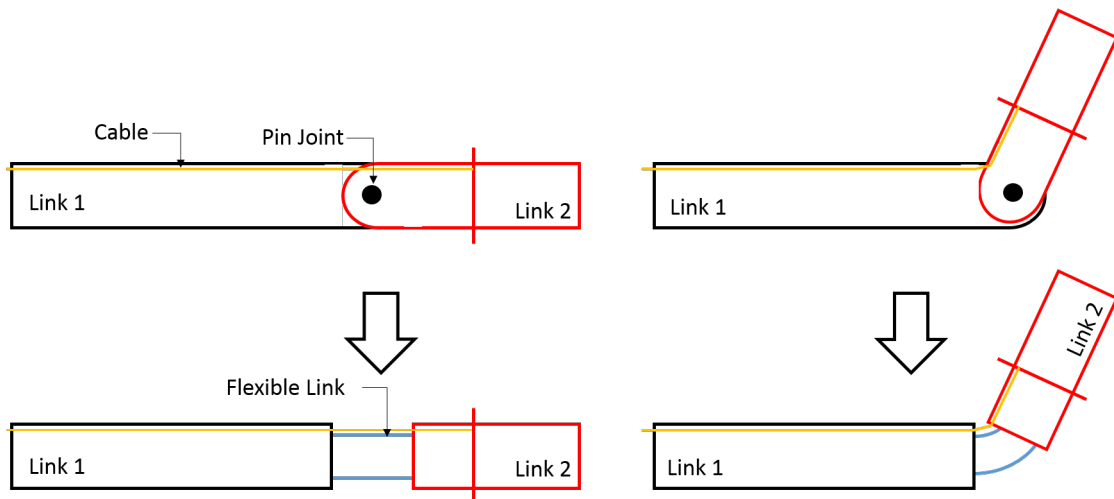
Figure 4.1. Pin joints replaced by flexible joints.

Pseudo-Rigid-Body models can be used to describe the behavior of the such flexible links. The 1 DOF and 2 DOF designs are shown below (Fig.4.2). Here, the flexible links are replaced by a pin joint and a torsional spring. The torsional spring would replicate the deflection path and force-deflection relationship shown by flexible links. The key for this assumption is the choice of placement of the pin joints and the value of the spring constants. The derivation shown here in this section, is from [13].
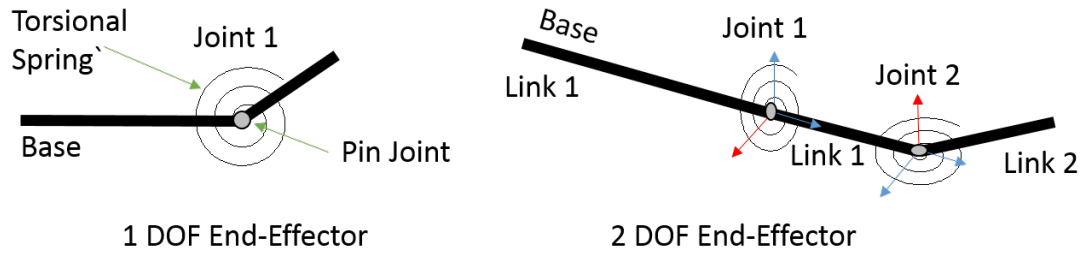
Figure 4.2.   Nerve retractor schematic.

For analysis, let us consider a simple one joint end-effector. The behavior of the flexible link can be compared to that of a small flexure-pivot. An example of a flexure pivot is given in Fig.4.3.
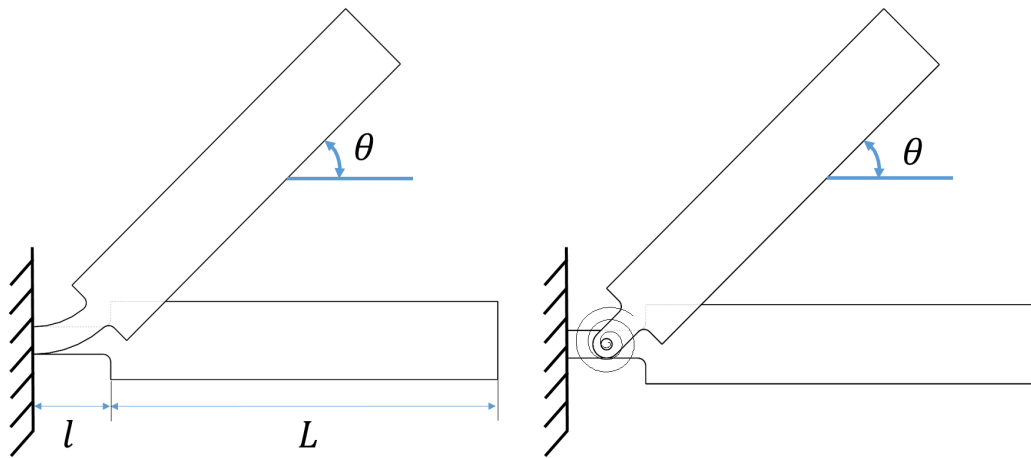
Figure 4.3.   Small flexure-pivot and pseudo-rigid-body model.

The main assumptions here are that the smaller segment is significantly smaller and more flexible than the larger segment. i.e.

$$L \gg l \tag{4.1}$$

$$(E_L I)_L \gg (E_l I)_l \tag{4.2}$$

where E_l is the Young's Modulus of the material of link of length l and E_L is the Young's Modulus of the material of the link of length L. The deflection equation for a flexible section with a moment the end is given by

$$\theta = \frac{M_o l}{EI} \tag{4.3}$$

where θ is the deflection of the link, and M_o is the moment at the end of the link, which gives the relationship between the moment and angle of deflection

$$M_o = \frac{EI}{l} \theta \tag{4.4}$$

or we can denote it in the form

$$M_o = k\theta \tag{4.5}$$

where k is the stiffness of the torsional spring

$$k = \frac{EI}{l} \tag{4.6}$$

This model is accurate only if bending is the dominant loading in the flexural pivot. The joint will be actuated using cables. The relationship between the tendon force and the deflection (under the assumption that there is no external load, and the axial force is insignificant) is given by

$$k\theta = rF \tag{4.7}$$

$$\frac{EI_l}{l}\theta = rF \tag{4.8}$$

It is to be noted that the performance of the pseudo-rigid-body models will depend upon the choice of stiffness of the joint and the choice of location of the pivot. For

convenience, the center point of the link is considered as the pivot. There is also a slight error in the pseudo-rigid-body approximation and the calculated deflection. The accuracy of the pseudo-rigid-body model is improved with smaller flexible link length.

4.1.2 Joint Kinematics

Considering the pseudo-rigid body model, we can propose a kinematic model for the nerve retractor by considering the geometry during bending. Since this is a generalized model, the pivot point is not considered to be at the center of the joint (Fig.4.4). We will also assume that the cables would remain in tension at all times.

The equations relating the angle of rotation of the join and the length of the cable used for actuation are derived as follows.
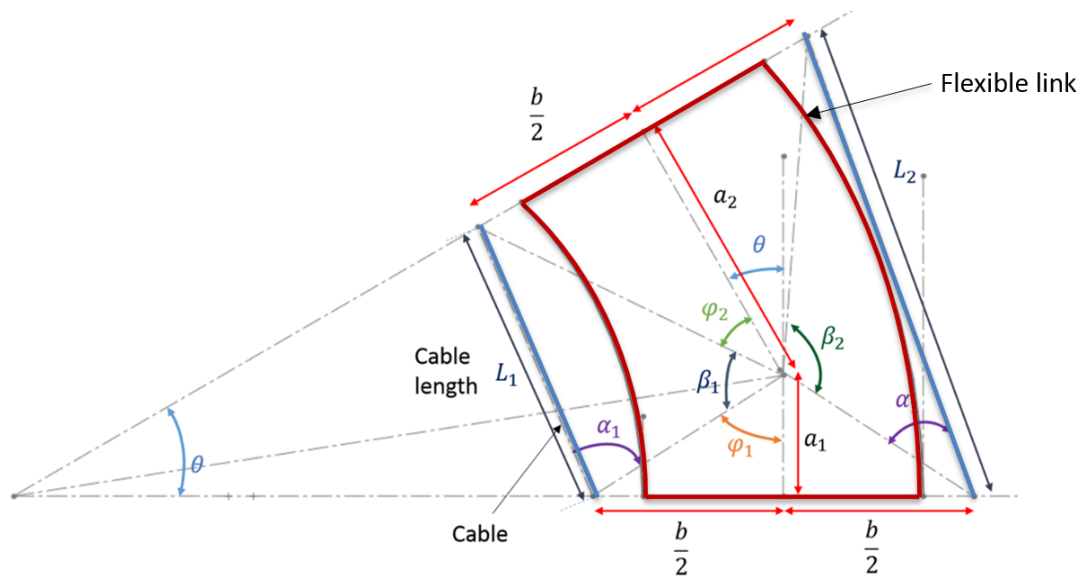
Figure 4.4. Joint model schematic.

Here, the length a is the length of the flexible link, and b is the width of the flexible link. Length a can be divided into a_1 and a_2 which are separated by the pivot

point. γ can be defined as the ratio between the length a_1 and a which can be used to denote the pivot of the link.

$$a = a_1 + a_2 \tag{4.9}$$

$$\gamma = \frac{a_1}{a} \tag{4.10}$$

The relationships ϕ_1 and ϕ_2 are given by

$$\phi_1 = tan^{-1}\frac{b}{2a_1} \tag{4.11}$$

$$\phi_2 = tan^{-1}\frac{b}{2a_2} \tag{4.12}$$

we can then derive value of α_1 and α_2

$$\alpha_1 = \frac{\theta}{2} + \phi_1 \tag{4.13}$$

$$\alpha_2 = \frac{\theta}{2} + \phi_2 \tag{4.14}$$

β_1 and β_2 are then given by

$$\beta_1 = \pi - \theta - \phi_1 - \phi_2 \tag{4.15}$$

$$\beta_2 = \pi + \theta - \phi_1 - \phi_2 \tag{4.16}$$

Now, using the sine rule, we can determine the length of the cable by

$$L_1 = \frac{\sin(\beta_1)}{\sin(\alpha_1)}\sqrt{\frac{b^2}{4} + a_2^2} \tag{4.17}$$

$$L_2 = \frac{\sin(\beta_2)}{\sin(\alpha_2)}\sqrt{\frac{b^2}{4} + a_2^2} \tag{4.18}$$

Hence the displacement of the cables required for the kinematics for a given angle θ is

$$L_1 = a - \frac{\sin(\beta_1)}{\sin(\alpha_1)}\sqrt{\frac{b^2}{4} + a_2^2} \tag{4.19}$$

$$L_2 = a - \frac{\sin(\beta_2)}{\sin(\alpha_2)}\sqrt{\frac{b^2}{4} + a_2^2} \tag{4.20}$$

a is the length of the flexible link and therefore, the initial length of the cable along the flexible link. L_1 is the length of the cable actuating the joint, and L_2 is the length of the other cable.

4.2 Grasper

4.2.1 Mechanism Design

Traditional graspers are mainly of two types. They can be classified as single jaw actuated graspers and double opposed jaw actuated graspers. In the single jaw grasper, one jaw is actuated, and the other jaw is simply fixed. The existing 3mm grasper is of this structure. A schematic of the mechanism is shown in Fig.4.5.
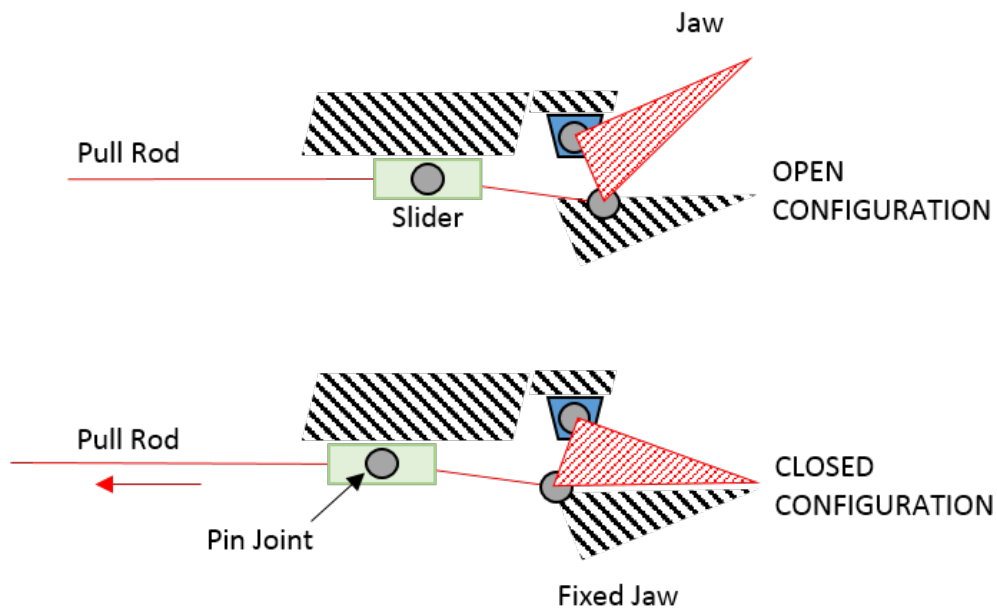
Figure 4.5. Mechanism for traditional single jaw grasper.

The two opposing jaw grasper, like the name suggests, use two separate jaws that come together to pinch the tissue. The mechanism consists of the two jaws pivoted about a fixed joint and actuated by a rhombus mechanism, where the jaws are the part of the rhombus mechanism (Fig.4.6).
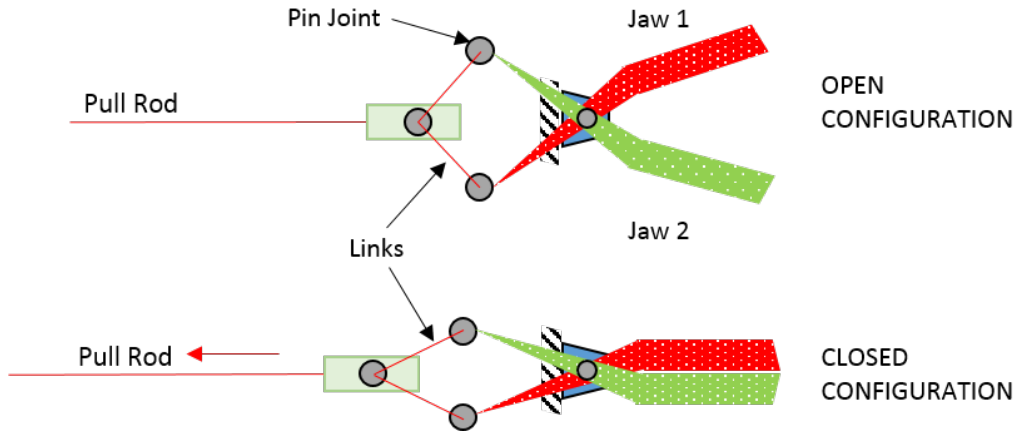
Figure 4.6. Rhombus linkage mechanism for double opposing jaws grasper.

4.2.2 Proposed Design

The proposed design for the grasper will take cue from the concept generation in Sec.4.1. The pin joints will be replace by flexible links.

The single jaw grasper would ideally have three flexible joints replacing the three pin joints. But all these flexible links won't be necessary since the cable used for actuation provides two pivot points that will complete the four bar mechanism. Only the pin joint holding the jaw to the base is replaced with a flexible link. The schematic is shown in Fig.4.7.

Similarly, the double opposing jaw grasper can also be designed with flexible links. Here, two such designs are presented. In the first design (Fig.4.8), all the pin joints are replaced by flexible links. This mechanism requires the flexible member to be strong to withstand the pull force.

Another prospective design is by eliminating the need to replace all the pin joints with flexible members and instead use the cable smartly to generate pivot points that can act as pin joints (Fig.4.9).
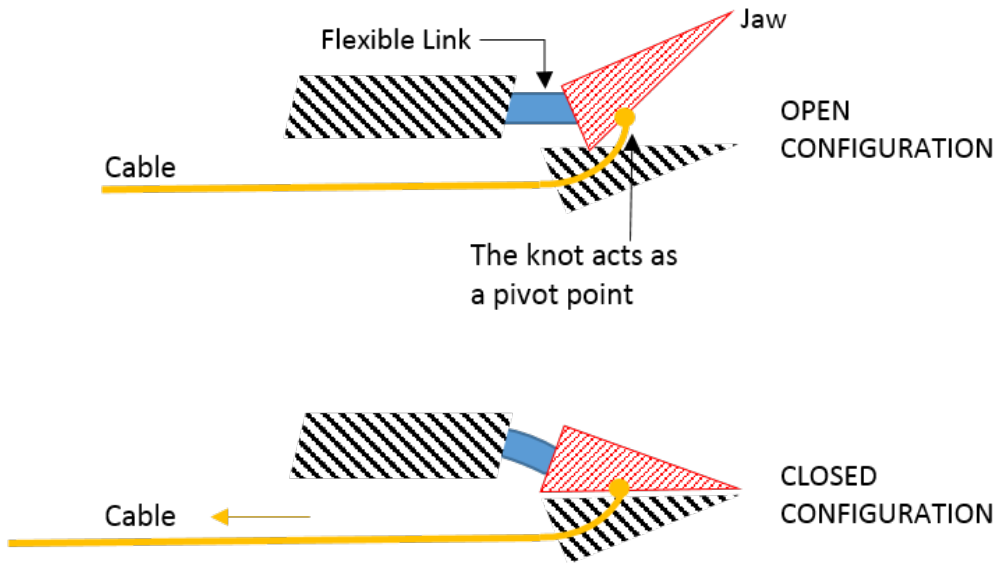
Figure 4.7. Compliant link grasper: Single jaw.
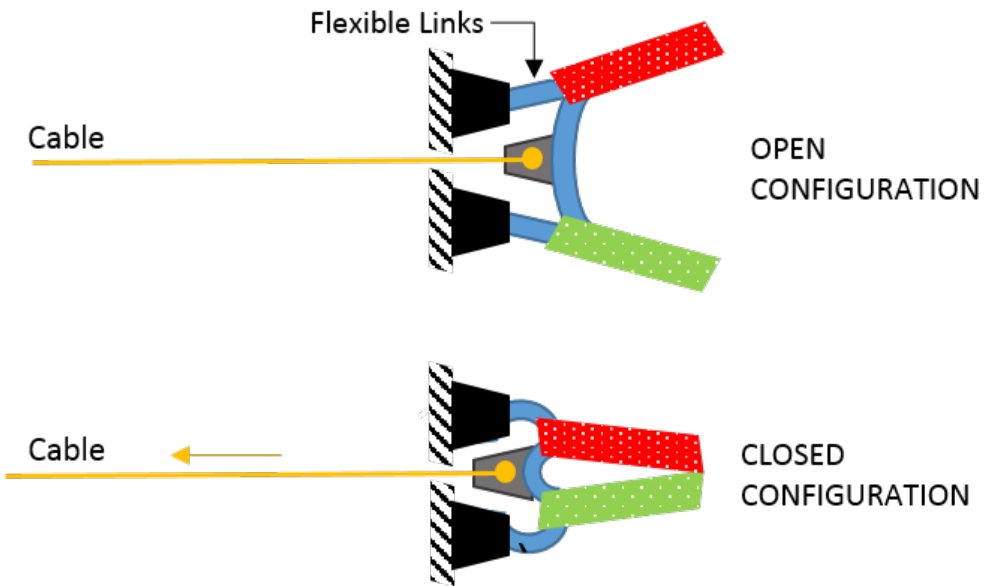
Figure 4.8. Compliant link grasper: Two opposing jaw, all flexible links.
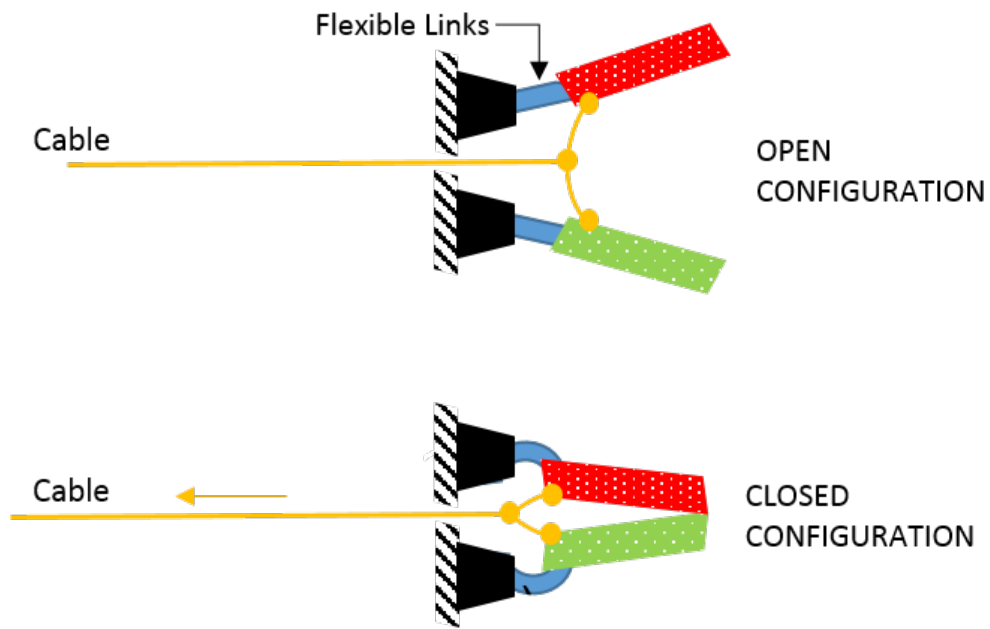
Figure 4.9. Compliant link grasper: Two opposing jaws, wire as pivot.

5. PROTOTYPE FABRICATION

The methods used for the construction of various components of the system are discussed here. It has to be noted that the materials selected for prototyping are not tested for surgery. These are just an embodiment of the proposed surgical system and further tests regarding its suitability for surgery have to be explored.

5.1 Cannula

The cannula is constructed using a 1' long 304 stainless steel tube (0.750" outer diameter and 0.065" wall thickness). There are multiple ports(holes) in the cannula for the insertion of instruments. The adapters are 3D printed and press fit into the ends of the tube. Special care has to be taken to align the ports during the fit. This can be done by using two shafts as a guide. The final assembly of the cannula is shown in Fig.5.1.
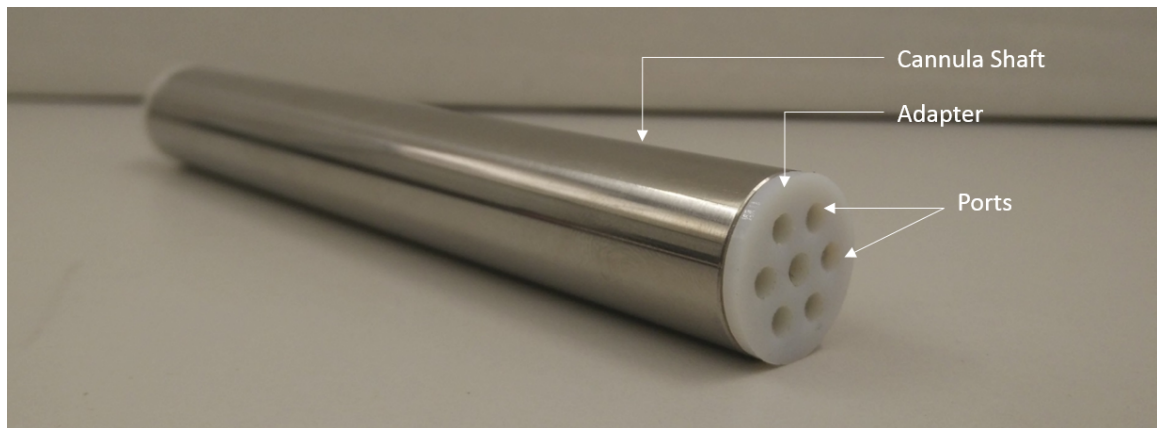
Figure 5.1. Cannula assembly.

5.2 Instrument Shaft Actuation System

The shaft is actuated for translational motion and rotational (roll) motion. For translational motion, it is required to support a maximum weight of about 300 g. An ACME lead screw with a Nema17 stepper motor is chosen for this actuation. The acme thread based actuation also ensures that the tool doesn't move due to the loss of power etc, while also providing enough torque for this application.

The actuator is a bipolar stepper motor (200 Steps/Rev, 1.7 A/Phase). The lead screw attached to the motor is 150 mm long and has pitch of 2 mm. The nut is made of bronze.

The required torque of the motor is given by [25]

$$T_d = \frac{PL}{2\pi e} \tag{5.1}$$

where P is the load (N), L is the lead of screw (m/rev), e is the ball bearing efficiency(0.25 for acme screws with bronze nuts), and T_d is the driving torque of the motor (Nm). Considering the load to be 1kg (10N), the driving torque required from the motor is 0.012732 Nm. Hence the Nema17 stepper motor (Rated holding torque : 0.36 Nm [28] POLOLU, Fig.5.2) can be used for this actuation. These actuators have significant backlash effects, but are sufficient since the surgeon would be able to adjust the position based on the visual feedback.

Figure 5.2. Nema17 motor with acme thread and nut.

The moving platform is attached to the lead nut and balanced by two linear slides on the side. The platform has four holes to faster the manipulator (Fig.5.3).
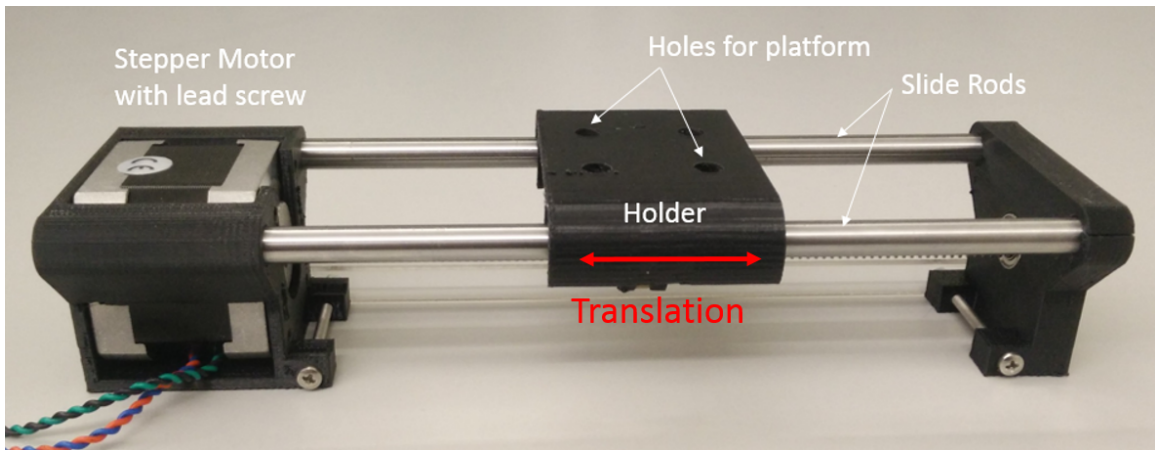
Figure 5.3.   Shaft actuation: Translation.
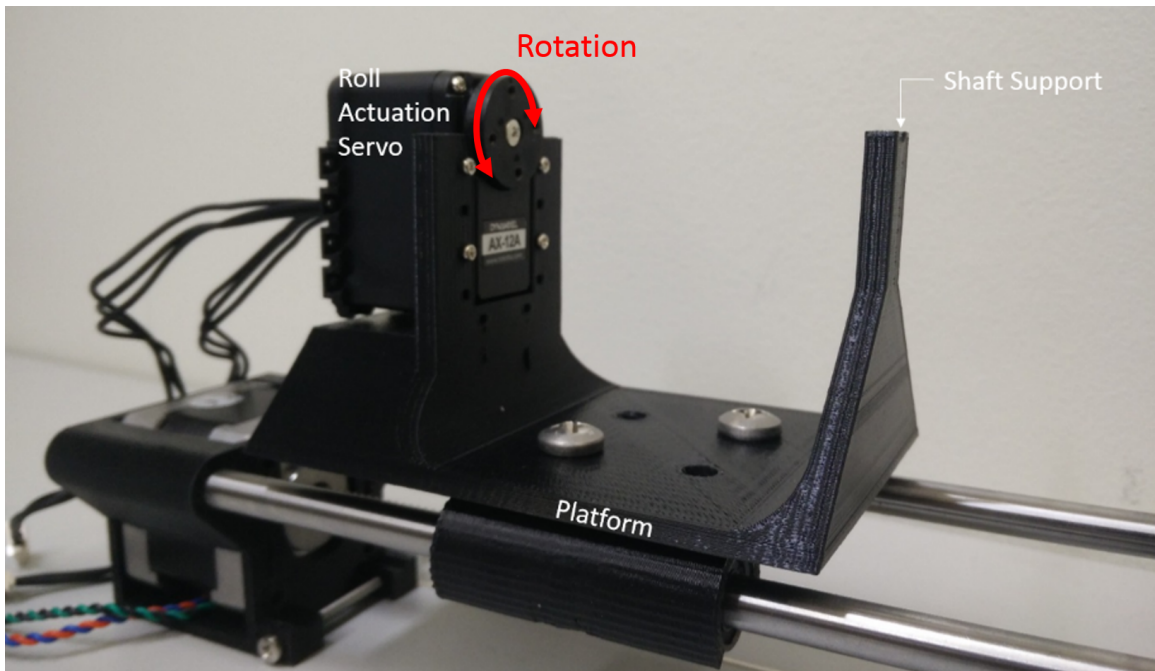
Figure 5.4.   Shaft actuation: Rotation.

The rotational motion (roll) to the shaft is provided by a servo motor (Fig.5.4). This motor rests on the platform and is aligned axially to the axis of the shaft. The stepper motor also carries the actuators used for the actuation of the end-effector.

5.3   End-Effector Joint Mechanisms

The proposed mechanisms in the previous chapter are considered for prototyping. The next aspect of the design was to choose an appropriate flexible link and propose steps for manufacturing. A variety of manufacturing and assembly processes were explored for this. These include assemblies with rubber tubes, casting of flexible members as joints between links and finally, 3D printed assemblies with flexible members.

5.3.1   Existing Elastomer Tubes

Rubber tubes from the market were used to assemble a manipulator. The tendon cable was attached to the end tube. The movement of the end-tube and the range were as expected (Fig.5.5)
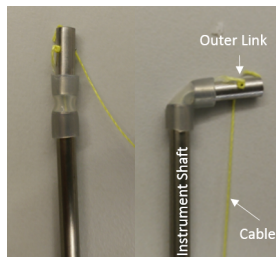
Figure 5.5.   Prototype with flexible rubber tube joint.

There were multiple issues with this design. There was no way of attaching the elastomer tubes to the long tube. On application of force, the elastomer tube used to slip out of the tube. Also, there were no smaller size tubes that could be sourced

to reduce the diameter of the joint. The next option was to use casting methods to make flexible joints.

5.3.2   Casting of Flexible Members

Two elastomers were considered for casting. This included the Simpact 60A urethane (Smooth-On Inc.;one part hardener and one part base) and laboratory grade PDMS (Dow-Corning, Sylgard 184; mixed one part hardener and one part base). Two methods were used here. The molds were fabricated using a desktop lasercutter;

For the construction of this mechanism, a technique caleld Laser Cut Elastomer Refill (LaCER)is used [40]. The steps required for this procedure is described in the Fig.5.6.
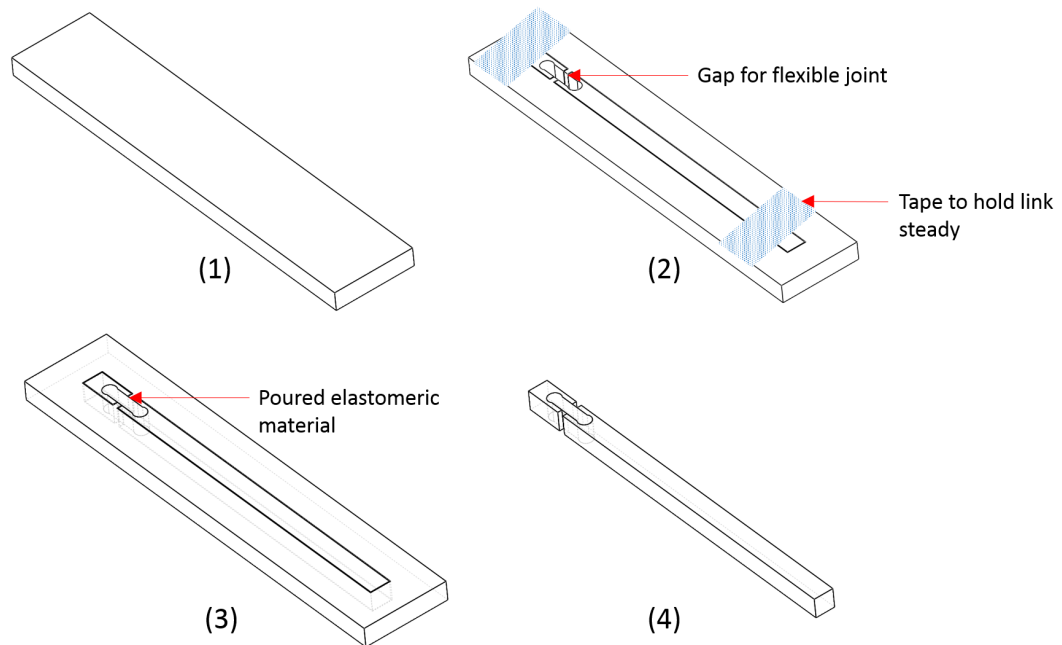
Figure 5.6. Steps for LaCER: (1)Plain acrylic sheet, (2)Lasercut part with gap for elastomer fill, (3)Curing of poured elastomer, (4)Mechanism removed from base.

Step 1: Prepare a sheet of rigid material which can be laser-cut

Step 2: Lasercut the pattern including the rigid links and flexible links on the sheet. Attach tape so that the rigid links do not fall off the cut set while it is being removed from the laser-cutter. The portion corresponding to the flexible link should be removed.

Step 3: Use another sheet of acrylic as base, and spray mold release before attaching the cut sheet on top of it using tape.

Step 4: Pour the prepared elastomer (PDMS) into the gap left on the laser-cut sheet. This elastomeric material is usually in its uncured form, degassed in vacuum and poured carefully into the gap for the flexible link. Excess elastomer material is removed from the surface.

Step 5: After the curing process, the mechanism can be removed from the base.

This is a quick method of prototyping 2.5D mechanisms, and allowed the ability to prototype different mechanisms with varying joint geometry and stiffness (Fig.5.7).
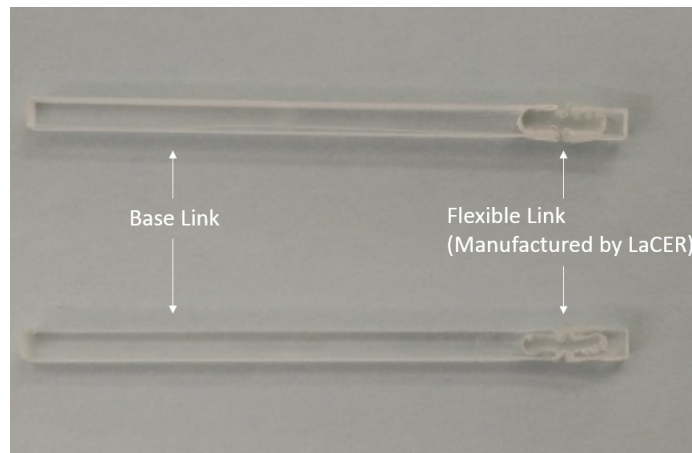
Figure 5.7. LaCER prototype

There are many issues with such design. There is a chance for the flexible link to slip out of gap due to insufficient sticking. There are difficulties in routing cables

to actuate the joint too. Also, the prototyping operation is not suited for mass production. Although there could have been variations in the experimental procedure here using different ratios of the hardener and base, this procedure is tedious and did not meet the requirement of the surgery.

Another method investigated was using 3D printers to cast 3D molds to generate paths for the cable actuation. Due to the small size restriction, it was difficult to get the elastomer fluid flow into the gaps of the newly designed mold. Alternatively, on testing a 3D flexible link made from Simpact 60A urethane (Smooth-On Inc.), it was found out that it lacked the elongation required for the joint. These drawbacks led to continued brainstorming for a new approach.

5.3.3   Multimaterial 3D Printed End-Effectors

Mutlimaterial 3D printers solved a lot of problems during manufacturing. It allows the creation of complex geometries and small features. The Connex Objet350 (Stratasys Ltd.) was chosen for this as this printer allowed the unique ability to print multiple materials as an assembly. Other printers considered were the Makerbot Replicator 2X (Makerbot Industries LLC.) and the Form 1+ printer (Formlabs). The makerbot based on fused filament fabrication and the form +1 based on stereolithography have flexible materials to choose from, but do not allow the printing of assemblies and support all at the same time. The comparison between the printers is shown in Table 5.1.

The Connex Objet350 printer (Stratasys Ltd.) was selected due to its resolution and accuracy, and the ability to print parts of different material as assemblies.

Table 5.1.   3D Printers Comparison.

Printer	LH (um)	MFS (um)	HR	MMA
Connex Objet350	16	20-85	Shore 40-95	Yes
Makerbot Replicator 2X	100	400	NA	No
Form 1+	25	300	Shore 80-90A	No

LH: Layer Height, MFS: Minimum Feature Size,

HR: Hardness of Flexible Material, MMA: Muliple Material/Assembly

5.4   End-Effector Design for 3D Printing

5.4.1   Flexible Joint Design

The cross-sectional view of the end-effector along the joint was taken into consideration. This sequence can be seen in Fig.5.8. The outer diameter of the end-effector is fixed at 3.175 mm. Next, the minimum wall thickness was determined to be 0.25 mm. For routing the tendons, the diameter of the channel was fixed at 0.6 mm. The last part to be fitted was the joint dimension.

The 1 DOF joint was designed with a rectangular cross section. The length of joint can be varied freely, but the limiting factor is the cross sectional dimensions. It was important to design the joint in such a way that the stiffness varies along the two planes to ensure deflection in a single axis. The Fig.5.9 shows the two dimensions, length A and width B.

The stiffness of the joint in *Plane X* is described as:

$$K = \frac{EI}{L} \tag{5.2}$$

where E is the young's modulus of the material, I is the area moment of inertia, and L is the length of the joint. I is given by

$$I_X = \frac{AB^3}{12} \tag{5.3}$$

$$I_Y = \frac{A^3B}{12} \tag{5.4}$$
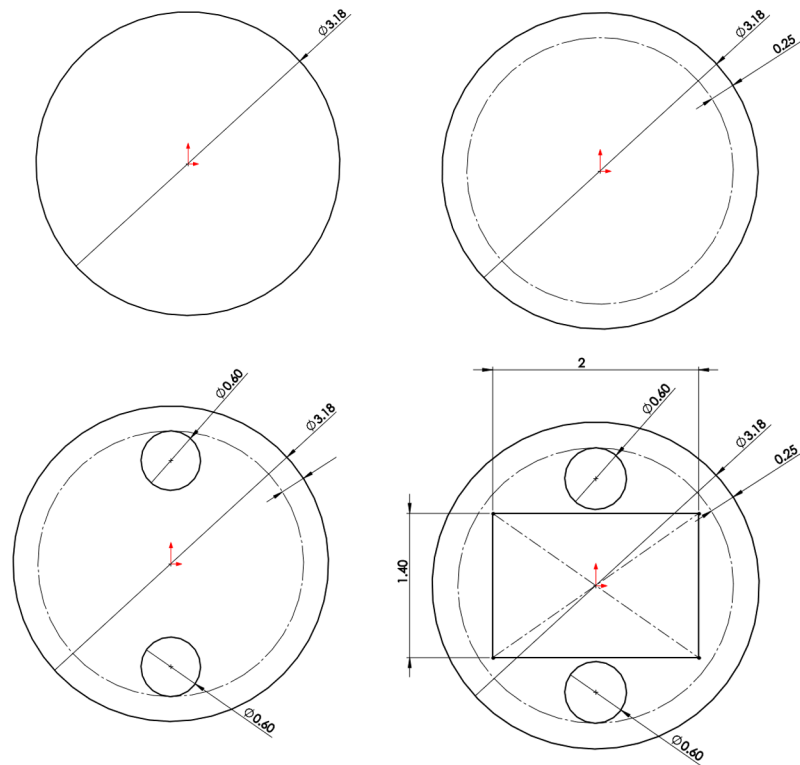
Figure 5.8. Cross-sectional view for joint design.
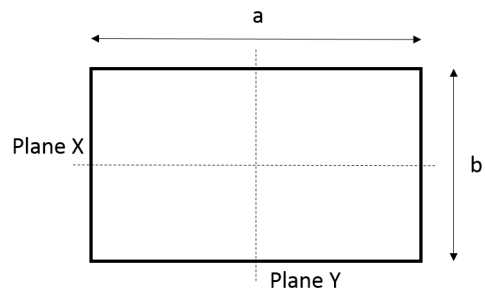
Figure 5.9. Flexible joint schematic.

Hence the ratio of stiffness of the joint is given by

$$\frac{K_X}{K_Y} = \left(\frac{B}{A}\right)^2 \tag{5.5}$$

To make sure that the stiffness is considerably lower on the actuation axis, it was decided to make the ratio of stiffness 1:2. Hence the dimensions chosen were $A = 2$ mm; $B = 1.4$ mm for the nerve retractor joint.

For the grasper joint, a similar design was implemented. Here, the single jaw of the grasper had to be actuated by the flexible joint. Since there is no need for routing of tendon near the joint, the entire width of the joint can be used. The cross section of the jaw is a semi-circle with diameter 0.125" (3.175 mm). The length of the joint was fixed to be similar to the nerve retractor and a suitable width of the joint was calculated, which came out to be 1.15 mm. The schematic of the actuated jaw is shown in Fig.5.10.
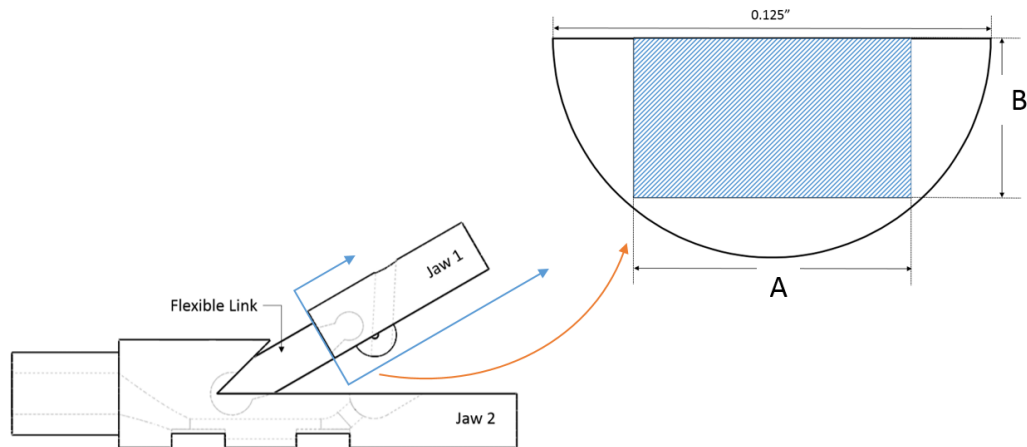
Figure 5.10. Flexible joint schematic for grasper.

Cable Routing: The cable chosen for the end-effector designs was the *Power-Strike Spectra Braided Fishing Line (20 pounds test)*. Braided wire was chosen for its low extension under load and the ease of knot tying. The diameter of the wire was measured to be 0.22 mm.

Fitting of End-Effector: The end-effectors are designed to be press fit into the insertion shaft. There is also channel designed to streamline the tendons from the sides of the end-effector to the center to be guided through the tube to the actuators.

5.4.2 Nerve Retractor Final Design

A blunt tip was chosen to prevent damages to the nerve/tissue due to accidental movement of the nerve retractor. The end-effector is also shaped conical to allow the positioning of the retractor between the compressed nerve and the disc material so that it can be retracted. This would allow for easy insertion of the retractor tip between the nerve and the disc material. Other considerations were to include ports between the cable channels for the provision to remove support material. **Final Design:** The final design of the end-effector is shown in Fig.5.11.
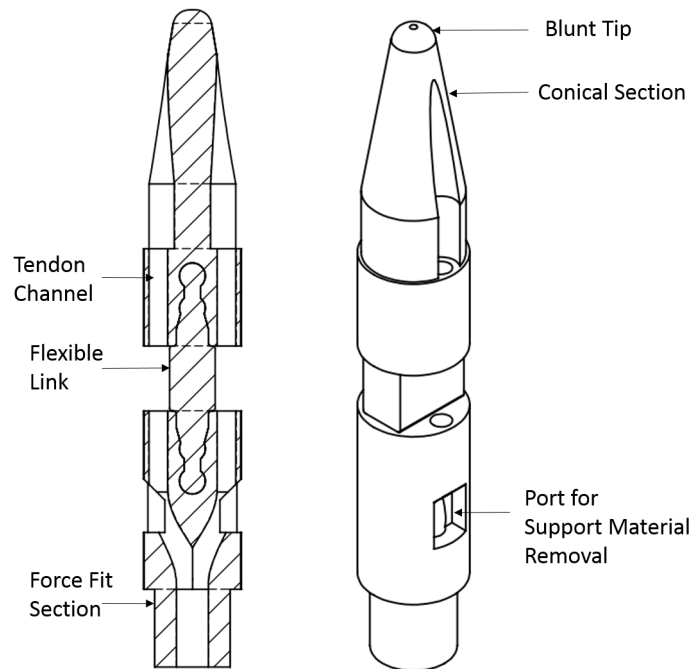
Figure 5.11. Nerve retractor design.

5.4.3   Grasper Final Design

Once the nerve retractor was successfully fabricated, it was clear what manufacturing technique was most suitable to building advanced mechanisms. Here, we discuss the manufacturing the grasper using the multi-material 3D printer. Both the designs discussed in Sec.4.2.2 were explored.

Final Design: The single jaw grasper was manufactured successfully using the 3D printer. A 1.15 mm wide flexible joint was used for the mechanism and the channels for cable routing were created to actuate the jaw to close on the other jaw (Fig.5.12).
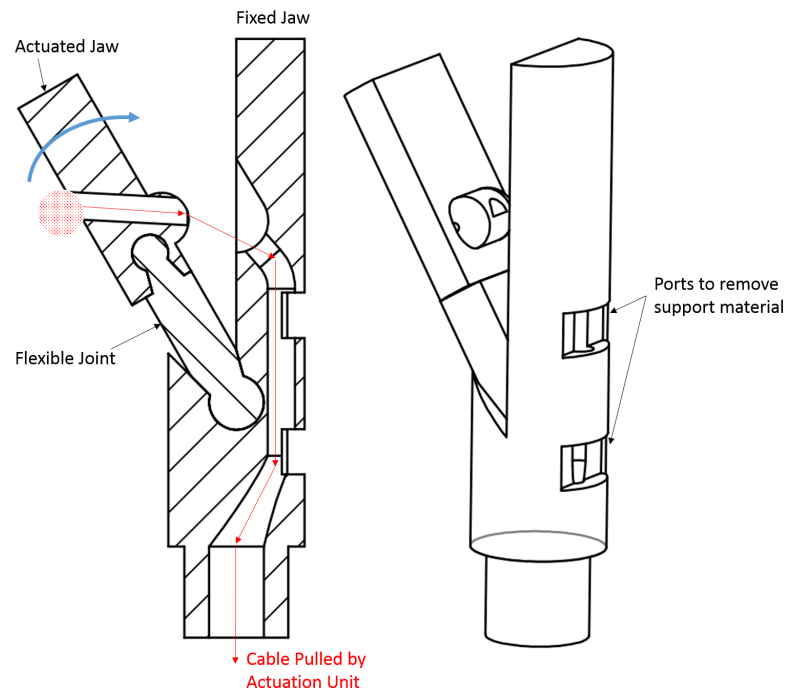
Figure 5.12.   Single jaw action grasper schematic and 3D printed part.

Double Opposing Jaw Grasper: The two opposite jaw action grasper designs designed in Sec.5.4.4 were fabricated successfully. But, these designs were not suitable for the project since the flexible links had to scaled down considerable to fit the mechanism in the constrained space, especially since the actuating tendons had to be

routed through the middle of the end-effector. This led to weak links and insufficient elongation. Another issue was that the wire couldn't be attached well enough to enable actuation forces which are required for the surgery. The printed pieces are shown in Fig.5.13. This design was not explored further due to the success of the single jaw actuated grasper.
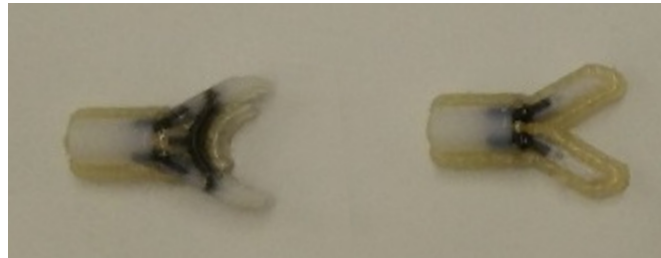
Figure 5.13. Double opposing jaw 3D printed parts.

5.4.4   Assembly Procedure

The multi-material printer prints parts with a washable support material. This material is often easily removed by high pressure water cleaner. But since our part is small, has flexible members, and thin features, it is advised not to use the pressure wash. The following are the steps that can be used to wash the part and clear the supports from the inner channels used for actuation.
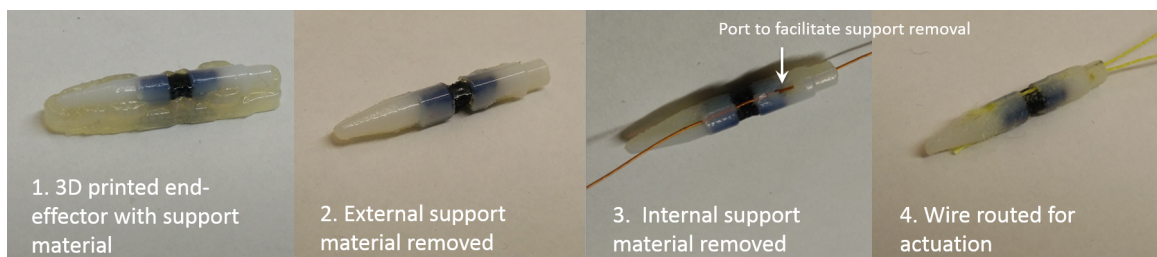
Figure 5.14. Assembly sequence nerve retractor.

1. The external support material are removed by breaking it off of the part. It can be rinsed in water to remove the coating around the part (Fig.5.14(1)).

2. Remove the support material around the outer end of the cable channels. Also, remove the support around the flexible link to access the channel.

3. First, use sharp need to push the support from one end of the channel. Then insert a 0.5 mm wire to remove the support material in the channel. This wire should be used to remove the supports from the intermediate ports facilitated for the support material. The supports would be removed through the ports or at places where there is a gap in the cable channel. It is advised to rinse it again at this point to wash away more of the support material (Fig.5.14(2)).

4. Insert a smaller 0.2 mm wire through the whole channel on each side to clear more of the support. Rinse the part again to remove support material (Fig.5.14(3)).

5. Route the cables through the channels (Fig.5.14(4)).

The assembly sequence, which includes the clearance of the support material and the routing of the cables are similar for both the nerve retractor and the grasper.

5.5 End-Effector Actuation Unit

5.5.1 Actuators

The actuation unit of the end-effector consists of two servos (Dynamixel AX-12) that have pulleys. These cable used to actuate the end-effectors are fastened to the pulleys. The servo motors allow for the controlled movement of the pulley. The servo motors can be used in an antagonistic fashion for a single joint to keep both the cables in tension. Or, they can be used to control two different joints, or a joint and an end-effector with a spring keeping the antagonistic cable in tension. The pulleys are mounted on a holder which is attached to the roll motion of the servo motor. The location of the pulleys is shown below.
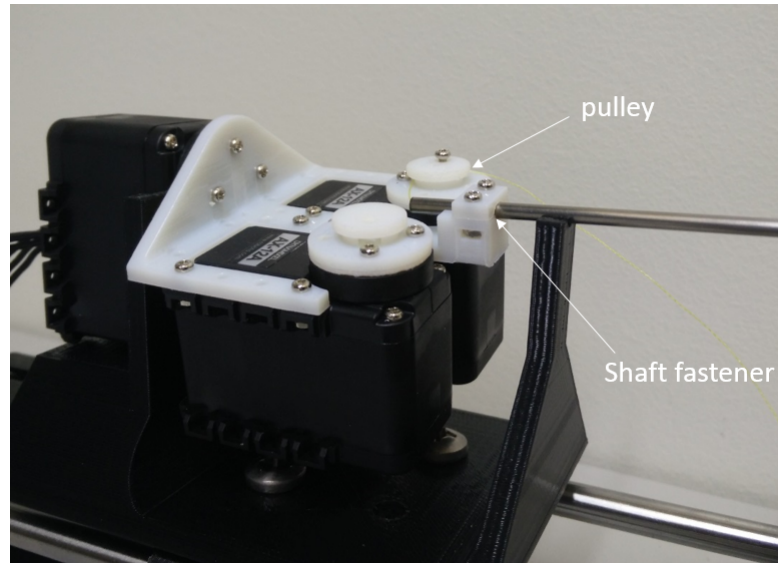
Figure 5.15.   Actuation Assembly.

After fastening the cable on the pulley, the pulleys are moved to tension the cable for actuation. The relationship between the pulling length of the cable and the angle of rotation of the pulley is given by

$$r\delta\theta = \delta L \tag{5.6}$$

where r is the radius of the pulley and L is the length of the cable being pulled.

5.5.2   Joystick

The joystick of choice for the surgeon is the Nintendo Wii nunchuk controller. This controller provides motion sensing in 3-axes and has two buttons, the Z and C button. The Z-button is used as a safety feature where the instrument is engaged only when Z is activated. The other keys can be used to control the movement of the manipulator through the surgeon who uses the feedback from the imaging setup to adjust the position of the manipulator.

5.5.3 Electronics

The dynamixel servos and the stepper motor for actuation are controlled by the Arbotix-M microcontroller (Fig.5.16). This micro controller dedicated ports to run and calibrate the servo motors. Also, the microcontroller has I2C available to implement the Wii nunchuk into the surgical system. The stepper motor is controlled by the micro-controller using a stepper motor driver (DRV8825, Pololu stepper motor driver, high current).
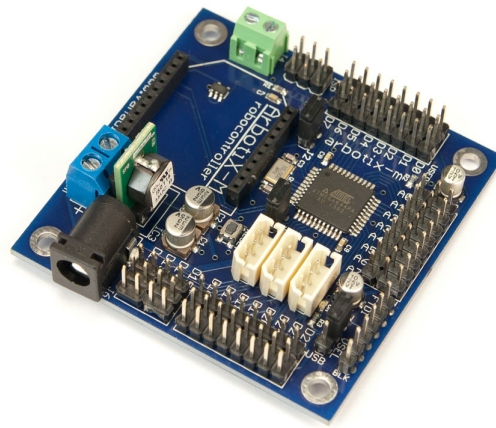
Figure 5.16.   Arbotix-M microcontroller [39].

6. RESULTS

6.1 Objectives

The objective of this section is to evaluate the capabilities of the system. This section will explore the force capabilities, and the proposed joint kinematics. For the nerve retractor, the parameters considered during the modeling are the flexible link length and the flexible link material. Link lengths of 1.8 mm, 2 mm, 2.5 mm, and 3 mm are considered. The materials that are considered for the flexible link are Shore 27, Shore 50, and Shore 70. These flexible materials are printed using a mixture of TangoBlack Plus, and VeroWhite materials in the Connex350 Multimaterial 3D printer. These materials are mixed in different ratios to obtain flexible links of required stiffness. The stiffness of the material can be ranked as $Shore27 < Shore50 < Shore70$.

6.2 Measurement Test Setups

The measurements required for the analysis are the angle measurement, and force exerted on the application of actuation load. In this section, the measurement test setups are discussed.

6.2.1 Angle Measurement

The size of the end-effector is too small to attach encoders to measure the rotation angles of the links. Hence, optical images were used to measure angles. For this, special end-effectors with fiduacial markers were fabricated, as seen in Fig.6.1. The markers are 1 mm diameter black circles 3D printed out of the soft material into the rigid portion of the end-effectors. These circles were used for tracking their positions

in Matlab. The centers of the markers were used to find the bending angle of the link. The line joining the markers at the base and the markers at the end of the end-effector are also used to find the PRBM joint location.
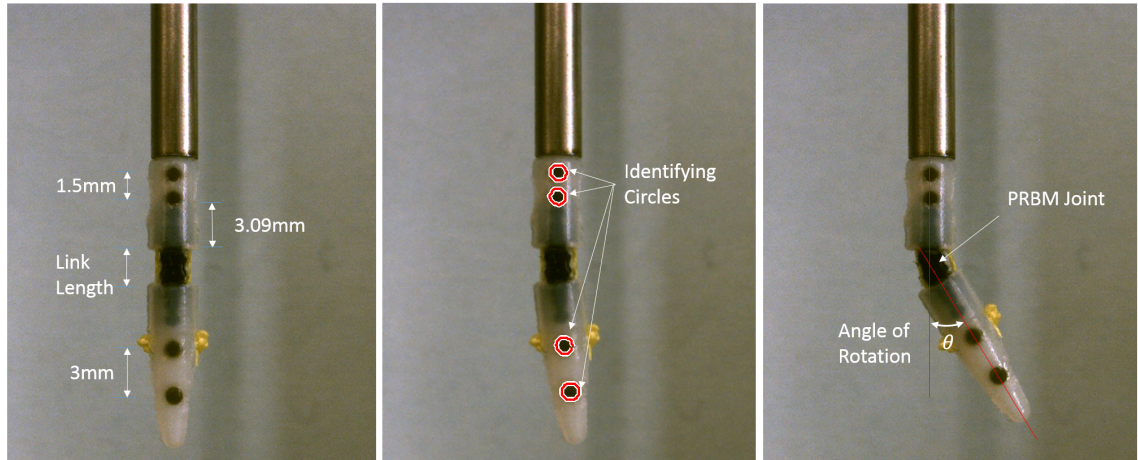
Figure 6.1. Angle measurement using Matlab.

The tendon displacements are measured using a single axis translation platform with a resolution of 0.001". The cables are fastened to the platform by clamping, using screw and nut. The complete setup is shown in Fig.6.2.

6.2.2 Load Measurement

The load measurement is done using a load cell (3132_0 Phidgets Micro Load Cell (0-780g)). This is connected to a bridge input (1046_0 PhidgetBridge 4-Input). The Phidget controller allows us to calibrate and measure the load on the cell. The loads used for applying forces are from the calibration weights set. They are attached using a noose knot. The complete test setup in shown in Fig.6.3. The actuation force of the nerve retractor and the clamping force of the grasper are measured.
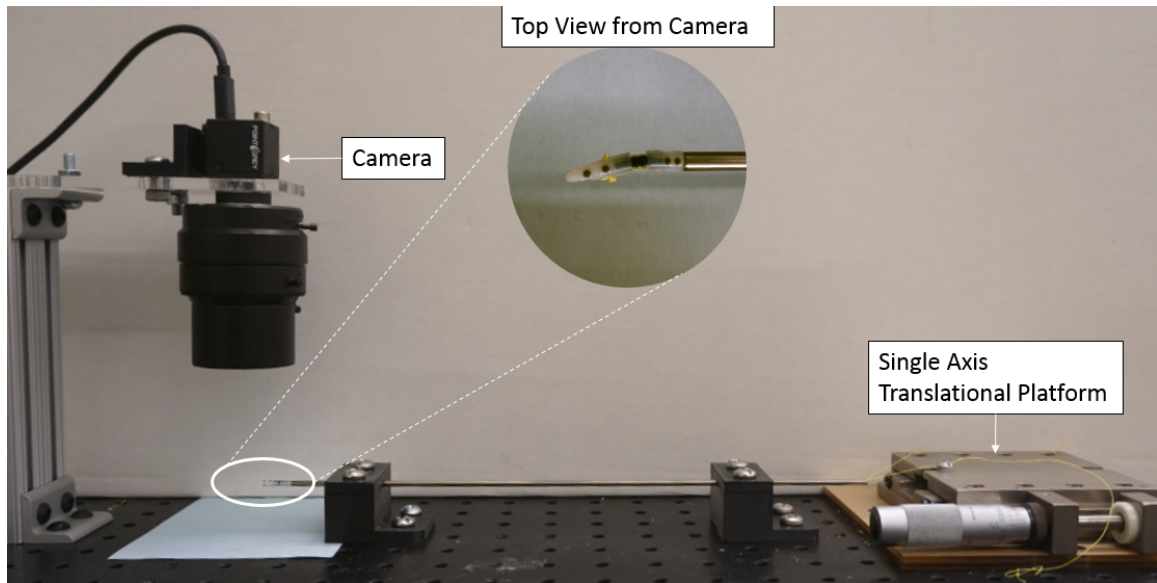
Figure 6.2. Test Setup for Measuring Angle.
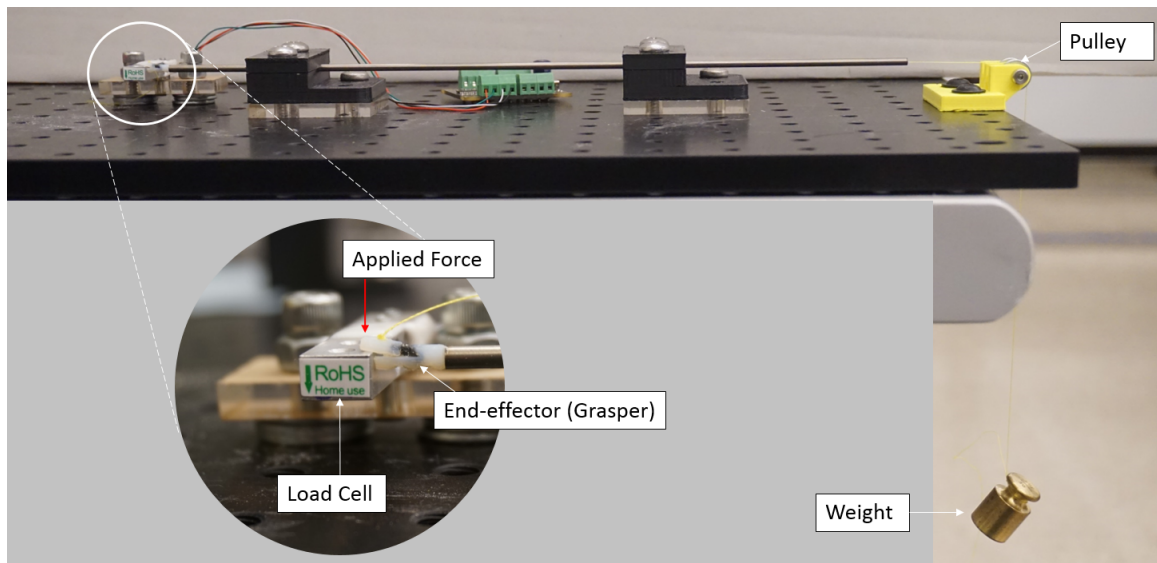
Figure 6.3. Test setup for load measurement.

6.3   Force Testing: Nerve Retractor

The force capabilities of the manipulator were investigated. The end-effectors with joints made of the three flexible materials, and flexible link lengths of 1.8 mm, 2.0 mm, 2.5 mm and 3 mm, were investigated. The force exerted on the cable was regulated and the load on the load cell was measured(Fig.6.4).
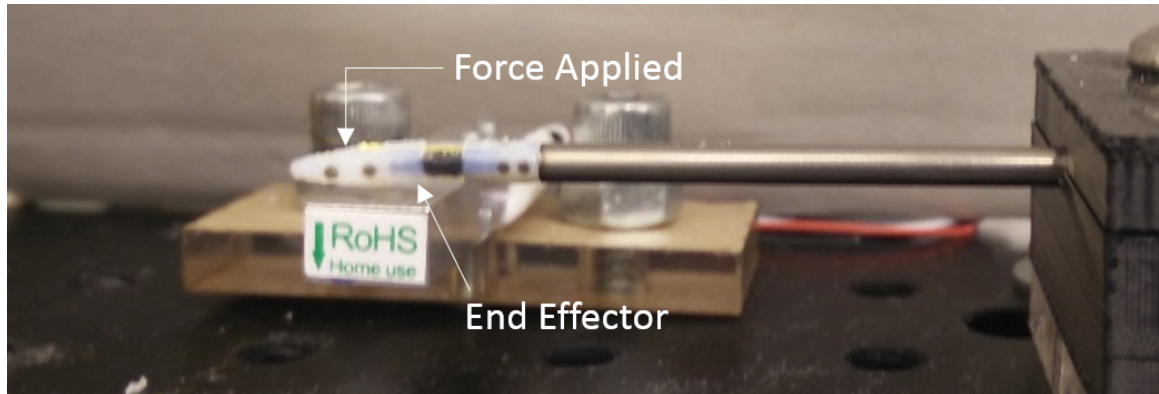
Figure 6.4.   Force measurement test setup.

6.3.1   Observations

A few observations can be made from the data in Table.6.1, Table.6.2 and Table.6.3

1. The forces generated for a particular cable pull force is constant across the varying flexible link material.

2. Tendency for buckling of the link is higher for longer links(Fig.6.5).

3. Only the 2.0 mm link with Shore70 hardness prevented from buckling at 500 g actuation force.

4. Highest force recorded was 52.82 g (.518 N).

Table 6.1. Retraction forces Shore 27 material flexible link.

Link Length Weight(g)	1.8 mm Force (mN)	2 mm Force (mN)	2.5 mm Force (mN)	3 mm Force (mN)
20	13.24	13.34	16.28	10.3
30	23.84	21.97	22.56	26.49
50	41.40	41.30	42.58	38.75
100	91.23	95.84	96.24	101.83
200	201.60	208.27	191.79	194.83[a]
300	302.74	345.51	302.34	303.03*
500	322.55	372.29	518.16	-

Force: Exerted force due to weight.

*Buckling of link.

[a]Severe twist of the flexible link.

5. The ratio of force applied on the cable to the force applied by the end-effector is approximately 10:1.

6. In one instance, the cable channel failed(Fig.6.5).
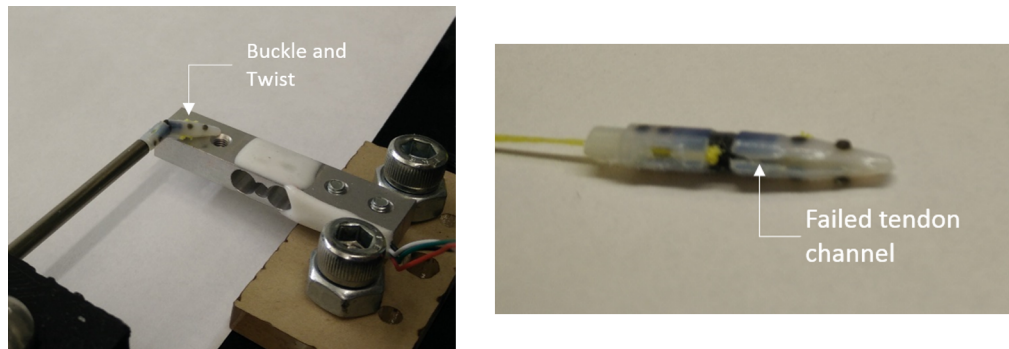
Figure 6.5. Failure during tests: Buckling of joint under actuation (Left) and Broken cable channels of end-effector (Right).

Table 6.2. Retraction forces Shore 50 material flexible link.

Link Length Weight(g)	1.8 mm Force (mN)	2 mm Force (mN)	2.5 mm Force (mN)	3 mm Force (mN)
20	11.87	15.30	12.75	12.26
30	22.17	22.86	21.68	21.58
50	42.87	41.10	43.75	38.95
100	94.67	91.92	92.02	84.76
200	190.41	191.10	177.27	127.92*
300	198.06*	245.05*	288.90	-
500	-	-	506.69	-

Force: Exerted force due to weight.

*Buckling of link.

[a]Severe twist of the flexible link.

6.3.2 Sources of Error

The following are a list of sources of error that can affect the measurements. They encompass few of the assumptions made during the experiment.

1. There is significant deviation in the transmission ratio for lower weights which can be attributed to the frictional forces in the channels.

2. The surface area considered for the measurement of force was difficult to control. The measured forces depend on this factor.

3. On application of excess force on the cable, the axial force component dominates over the pure moment assumption. This leads to the buckling of the joint.

4. The wear on the flexible joint would take its toll during the experiment which could lead to tendencies in buckling. Here, pre-load is definitely a factor, and could have influenced the parameters.

Table 6.3. Retraction forces Shore 70 material flexible link.

Link Length Weight(g)	1.8 mm Force (mN)	2 mm Force (mN)	2.5 mm Force (mN)	3 mm Force (mN)
20	0	0	16.87	21.78
30	0	14.62	31.39	36.10
50	22.86	34.73	51.40	58.37
100	72.30	88.09	118.60	99.77
200	190.80	199.83	191.79	156.47
300	263.10	298.81	302.34*	257.22
500	Fail	434.19*	376.70*	458.13*

Force: Exerted force due to weight.

*Buckling of link.

[a]Severe twist of the flexible link.

5. The weight of the end-effector is considered negligible.

6.3.3   Conclusions

The following conclusions can be made from these tests.

1. There is sufficient force for manipulation of soft tissues. Under 5 N (500 g force) of actuation force, there is a force of about 0.5 N observed, which is higher than the required 0.35 N force (Sec.3.3.1)

2. Low stiffness end-effectors can be used in situations where the application of high force can be risky. Their max force before buckling is 0.3 N (30 g force)

3. Further studies should be used to relate the relationship between force of actuation in cables and measurements across the length of the manipulator

6.4 Force Testing: Grasping Force

The clamping force of the manipulator was measured by loading the tendon and measuring the force exerted by the jaw on the load cell(Fig.6.6). A special end-effector with a shorter jaw was used for this test. Only one flexible material(Shore 50) was used for this test, because of its medium stiffness and elongation properties. The higher stiffness materials (Shore 70) tend to have lesser elongation and lower elongation materials (Shore 27) are not stiff enough to hold the jaw.
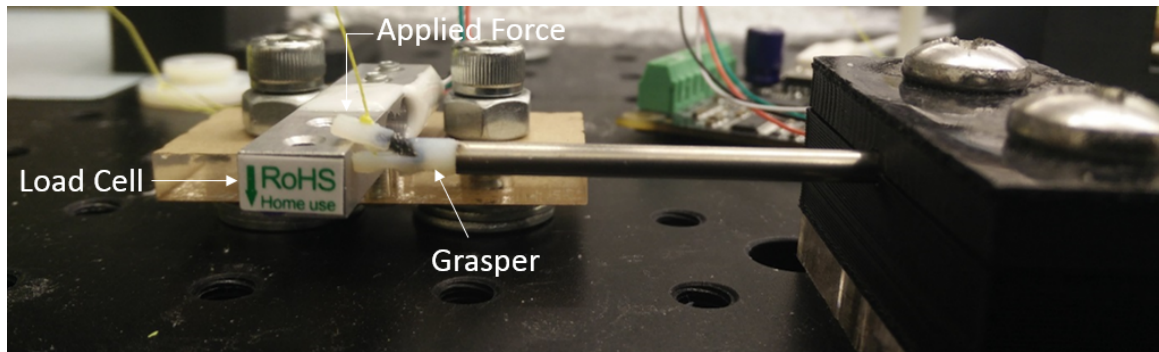
Figure 6.6. Clamp force measurement test setup.

Table 6.4. Grasping forces for Shore 50 material grasper.

Weight Applied (g)	Grasp Force (mN)
20	53.4
30	79.6
50	168.3
100	338.9
200	572.2
300	722.6
500	1232.6
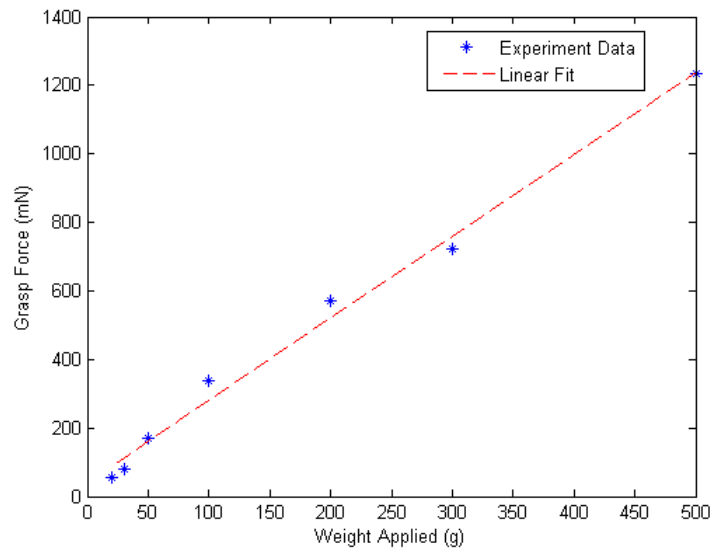
Figure 6.7. Graph of grasp force.

6.4.1 Observations

The following observations were made from the tests.

1. The clamping force has an approximate linear relationship between applied load and clamping force (Fig.6.7).

2. There was no failure of the grasper flexible link on application of high load.

3. The maximum load applied was limited to the ability of the test setup to hold the weight. On application of high load, there was significant slip between the instrument shaft and the fixture, which limited the application load.

6.4.2 Sources of Error

The sources of error for this test are

1. The friction in the cable channels could affect the readings.

2. The instrument shaft could slip from the fixture during application of high loads.

3. The area of contact of the joint could vary between readings due to instrument shaft slip.

6.4.3 Conclusions

The following conclusions can be made from these tests.

1. The designed grasper exhibited a clamp force of about 1.232 N at 500 g applied load. This is higher than the requirement of 0.2 N (Sec.3.3.2).

2. There was significant clamping forces for the grasper. This value can be considered comparable to the existing graspers due to their similar mechanical advantage.

3. The flexible link didn't show much fatigue during the tests, even at higher loads.

4. The transmission ratio of the grasper is much higher than that of the nerve retractor. This might be useful to consider for future re-design of the nerve retractor for higher forces.

5. Future studies can test the pull force of the end-effector which will give a better idea about the capability of this end-effector as a grasper.

6.5 Joint Kinematics

The kinematics of the joint discussed in Sec. is investigated here. The settings in which the experiments were conducted are as follows.

1. There is no external force on the end-effector during the test.

2. The experiment is conducted for flexible link lengths of 1.8 mm, 2 mm, 2.5 mm and 3 mm. The flexible link is of Shore50 material.

3. The controlled tendon is length is varied in 0.005" increments.

4. Only one cable length is controlled. The other cable is tensioned with a 10 g weight.

The following assumptions were made for this experiment.

1. The parameter γ used for modeling is adjusted for each link length to find a close fit with the experimental data.

2. The value of the distance between the cables (b) is fixed at 2.6 mm.

6.5.1   Experimental Results
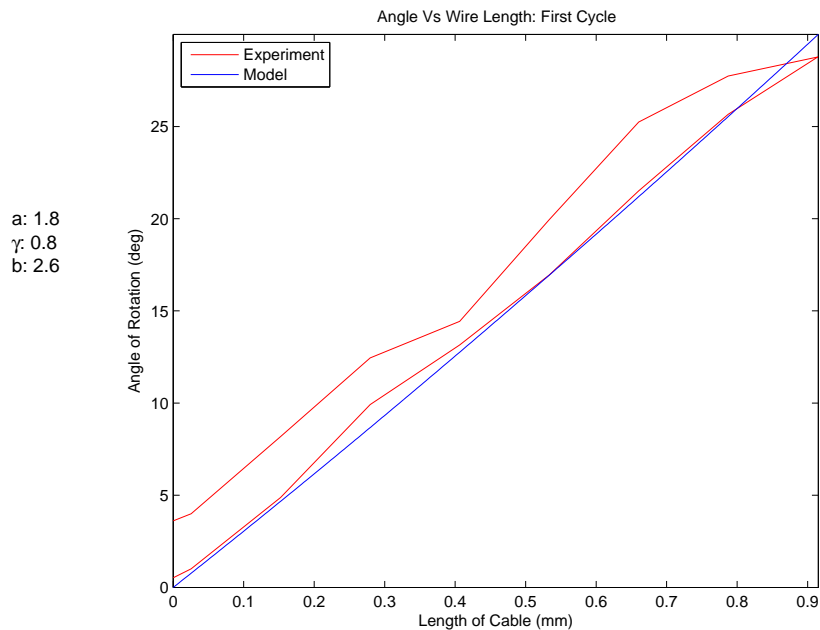
Figure 6.8.   1.8 mm Shore 50 material joint.

The kinematic modeling was tested out here. Graphs detailing the rotation of the end-effector vs the pull length of the cable were generated, and are shown in Fig.6.8to Fig.6.11. These plots show the behavior of the end-effector from a deflection of $0°$ to
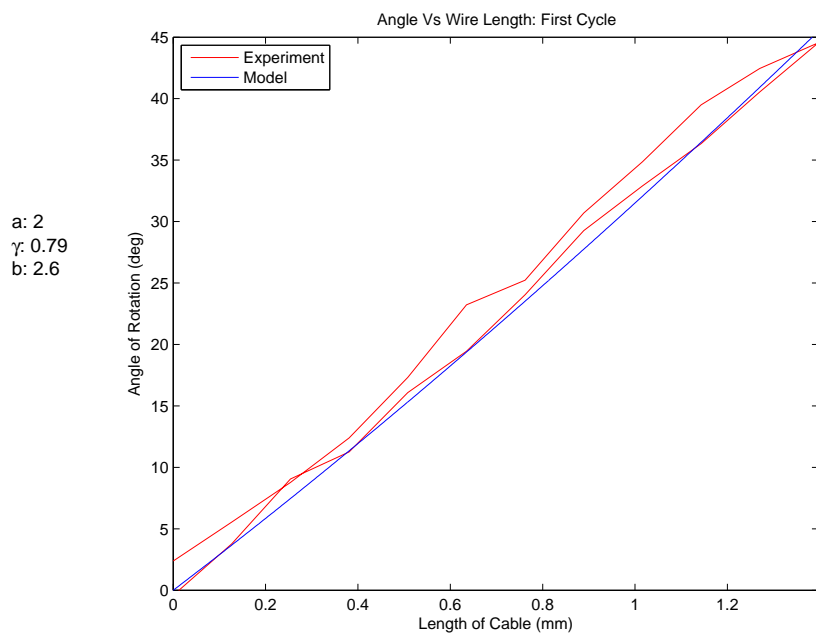
Figure 6.9.   2.0 mm Shore 50 material joint.
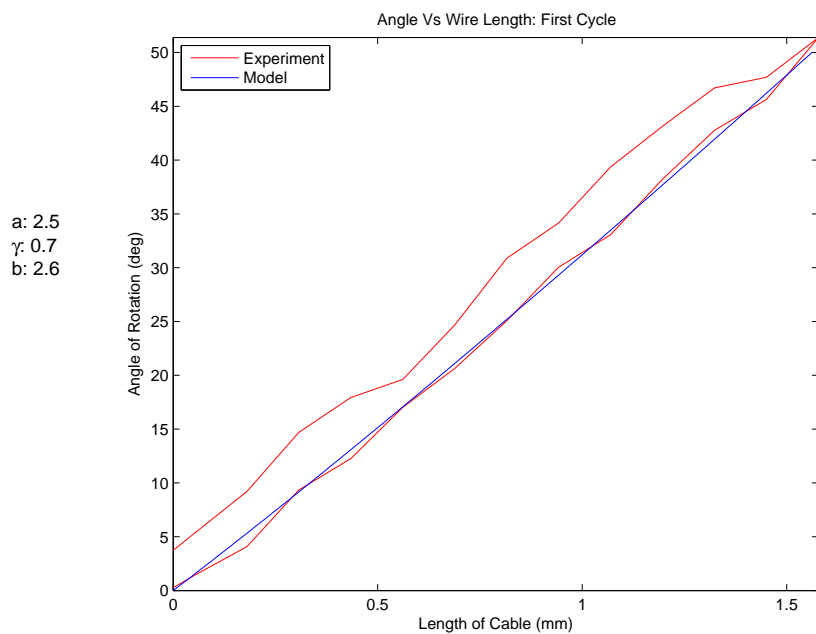
Figure 6.10.   2.5 mm Shore 50 material joint.
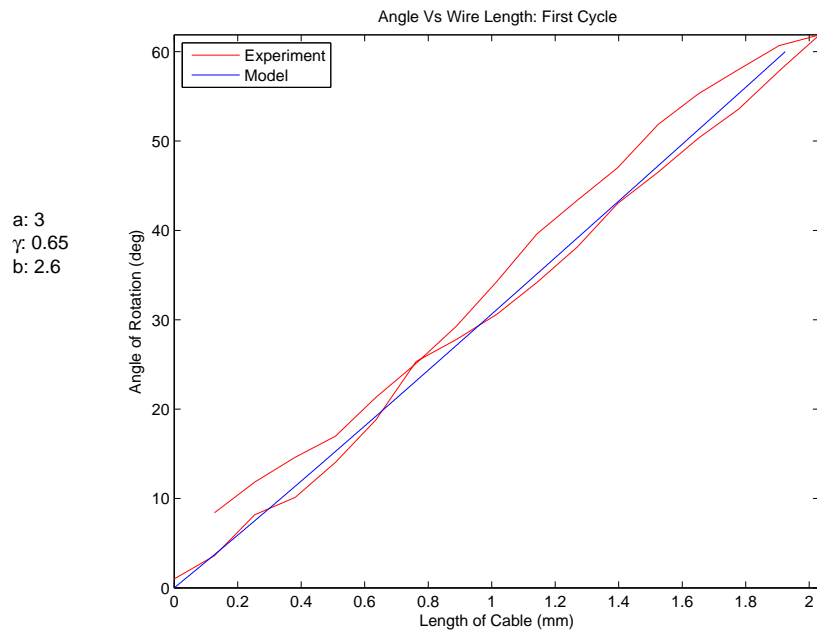
Figure 6.11. 3.0 mm Shore 50 material flexible link.
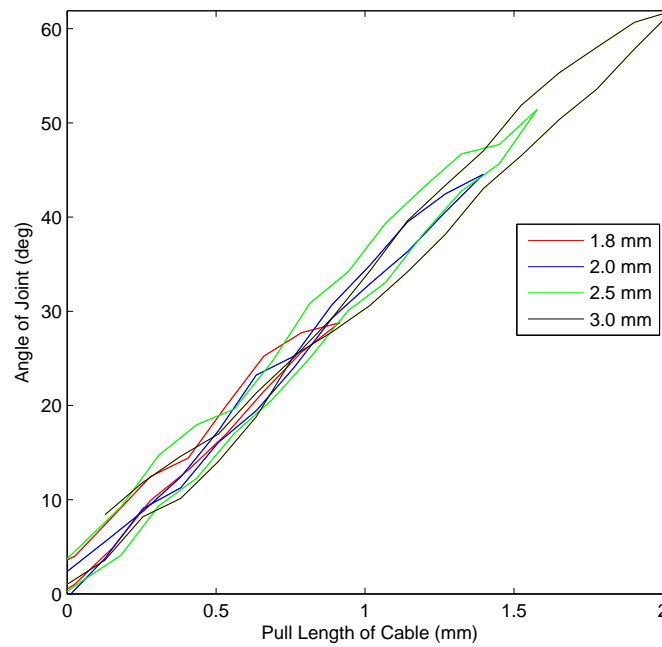
Figure 6.12. Comparison of all joints.

its recommended range and then back to 0°. A graph to compare the movement of the nerve retractors of the different lengths are shown in Fig.6.12.
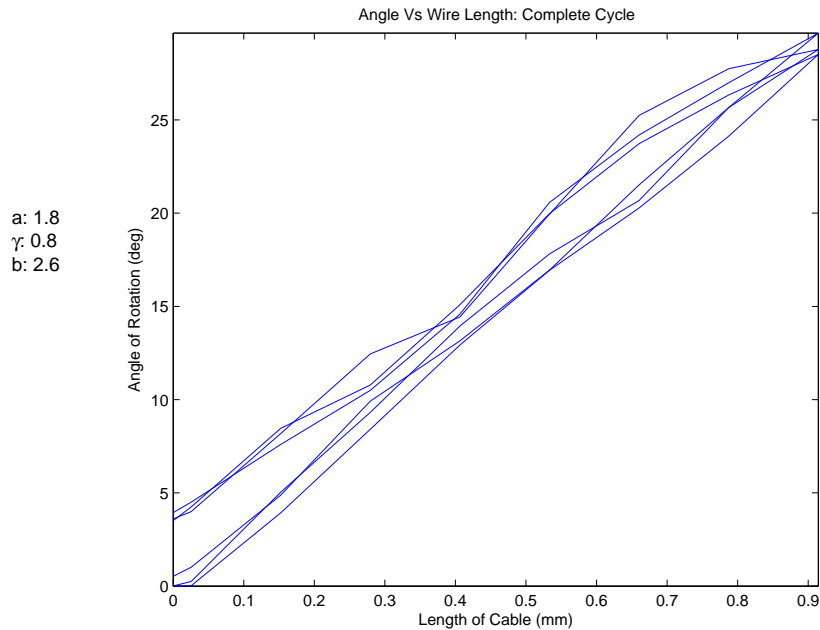
Figure 6.13. 1.8 mm Shore 50 material joint, repeatability test for 3 cycles.

The behavior of the joint after repeated rotations was also investigated to study its repeatability(Fig.6.13 to Fig.6.16). The actuation was repeated for three loops and the change in angles were recorded.

6.5.2 Observations

A few observations were made from the experiments.

1. There is hysteresis in the rotation of the flexible link. It amounts to maximum of 13.33% on 1.8 mm link and 5.55% on the 2.0 mm link.

2. The value of γ for the kinematic model is higher for shorter links.

3. The range of motion of the end-effector is higher for longer flexible links.
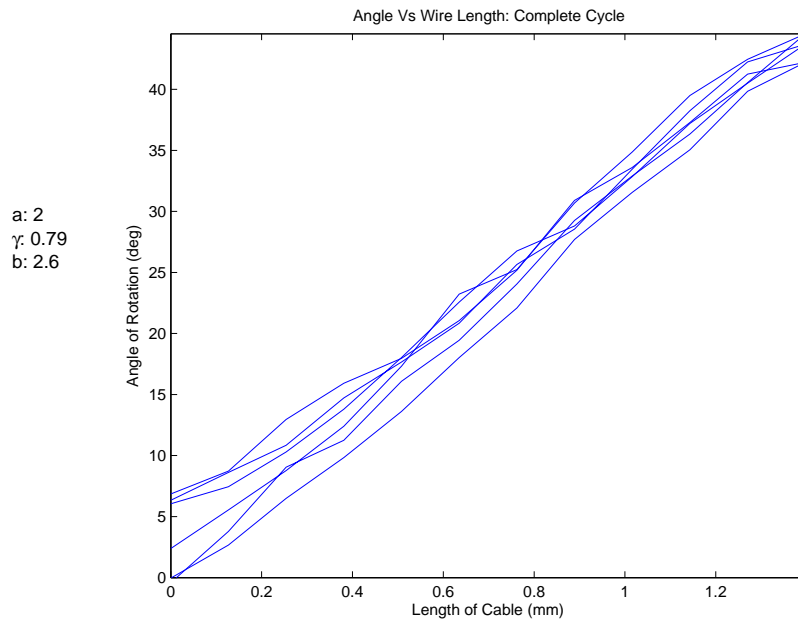
Figure 6.14.   2.0 mm Shore 50 material joint, repeatability test for 3 cycles.
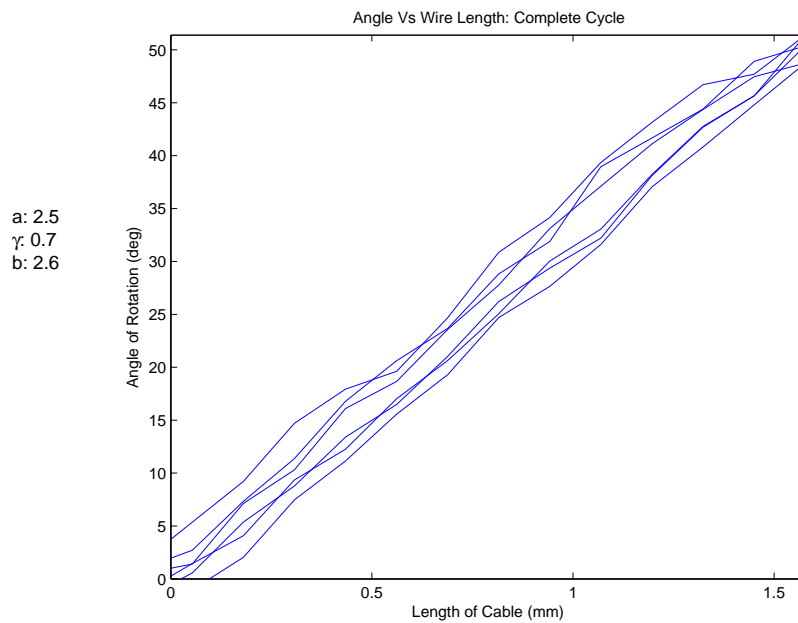
Figure 6.15.   2.5 mm Shore 50 material joint, repeatability test for 3 cycles.
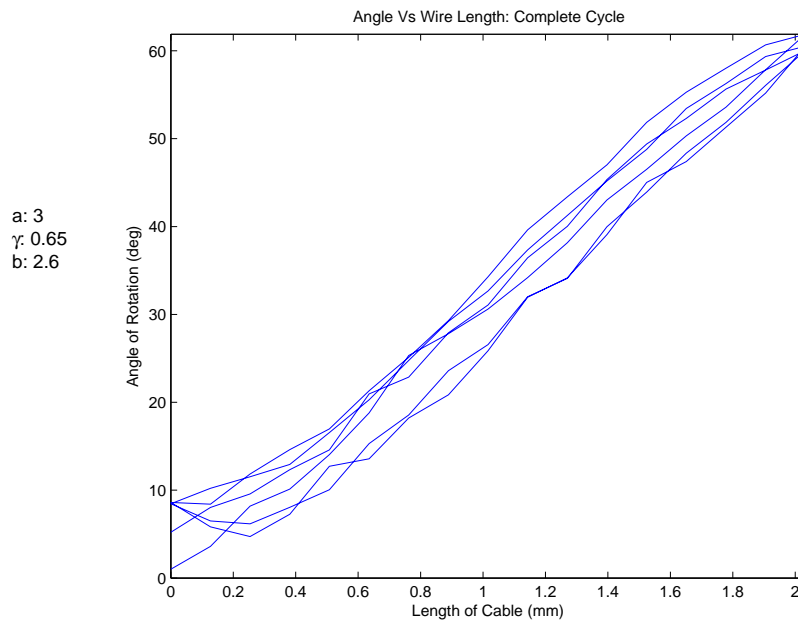
Figure 6.16.   3.0 mm Shore 50 material joint, repeatability test for 3 cycles.

4. The repeatability of the mechanism is $\pm 3°$.

5. The permanent deformation of the flexible link is about $4 - 5°$.

6.5.3   Sources of Error
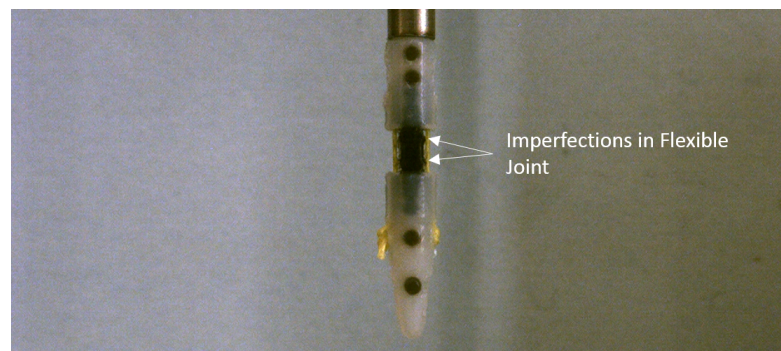
Figure 6.17.   Imperfections in 3D printed part : 3.0 mm Flexible Link.

The following are a list of sources of error that can affect the measurement. They encompass few errors that creep in due to the assumptions made during the experiment.

1. The geometry of the joint is not perfect (Fig.6.17). This is attributed to the deposition of support material during the 3D printing process. This can lead to changes in the PRBM-joint modeling.

2. Deformations in the cable channel during actuation.

3. Change in lighting conditions during the capture of images can affect the identification of centers of the markers. This may affect the angle measurements.

4. The counter force provided by the 10 g weight could be less, and hence might have affected the response of the flexible link which could lead to the hysteresis.

6.5.4 Conclusions

1. The trend of the experiments match that of the proposed model.

2. Long flexible links have higher tendency for the imperfection in the flexible link because of the gap in between the support material.

3. Short flexible links have limited range of motion($< 30°$).

4. Flexible link length of 2.0 mm or 2.5 mm are suitable for this end-effector.

5. Strong counter forces on the other cable may be required to prevent the effects due to hysteresis.

6. Further studies should be considered to study the effects of friction in hysteresis too.

7. CONCLUSIONS AND FUTURE WORK

7.1   Conclusions

The proposed system has the required capabilities for performing the surgery. This system combines the positive aspects of both MED and AMD. With smaller incision compared to MED, there is the scope of designing a manipulator with articulated end-effectors that can provide the required dexterity for the surgery. The ability to use multiple instruments at a time will make the job of the surgeon much easier. If required, the end-effectors can also be designed to work together to do the same task which further augment the force capabilities of the manipulator. Alos, since the manipulators are made using flexible members which have their limits in the application of forces before they buckle, they could be designed to limit the force capability to safe levels. This will prevent injury due to accidents or control errors during the surgery.

The endoscope can now be adjusted by using different ports during the surgery. This will limit the movement of the trocar during the surgery. Further, the endoscope can be attached to an end of a 1 DOF manipulator for articulated movement in the surgical workspace improving the field of view for the surgeon.

Another aspect of 3D printed designs is the cost. The end-effectors tested here can be 3D printed in large numbers in a short period of time. Although they require assembly, it will challenge the existing instruments in the market, because of its simplicity and effectiveness. The forces required for the surgery are achievable with the designed end-effector and these preliminary designs can be extended to design articulated end-effectors. We have displayed a proof of concept of a 1-DOF joint (Nerve retractor) and a grasper. In future, we can create articulated graspers that will provide added dexterity in the workspace. There is also a possibillity of scaling

these designs for achieving larger forces and reliability, especially in cases where there is no tight limitation in the instrument diameter.

Sterilization of these instruments through conventional techniques like autoclaving is not possible due to the low melting point of these materials. But, since the cost of manufacturing is low, these instruments can be designed to be disposable after use. Lastly, since the materials used in this design of the end-effector is mainly plastic and rubber, they can be considered for use in surgeries under the presence of MRI, with minor changes to the materials used for the instrument shaft actuation and other actuators.

A summary of features of the proposed system and the existing types of surgeries are shown in Table.7.1.

The performance of the designed tools were also measured. They were compared to the design requirements and were found to be adequate for the tasks that they are required for during the surgery. A summary of results are given in Tab.7.2 and Tab.7.3.

The final assembly of a manipulator is shown in Fig.7.1.
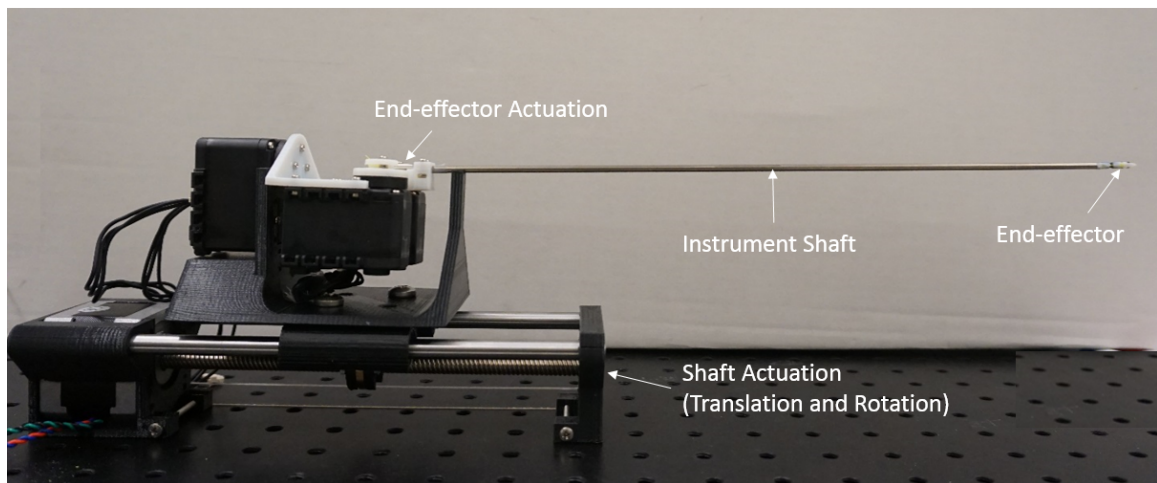
Figure 7.1. Final assembly.

Table 7.1. Surgical instrument comparison and target design specifications.

Features	Open	MED	Arthroscopic	Proposed System
Manipulator Type	Articulated	Rigid	Rigid	Articulated
Manipulator Material	Rigid	Rigid	Rigid	Flexible
Workspace Size	Large	Medium	Small	Medium
Control	Manual	Manual	Manual	Teleoperated
Required Incision Size	40mm	24mm	5-10mm	18mm
No. of Manipulators	Multiple	One	One	Multiple
Cooperative Manipulation	Yes	No	No	Yes
Endoscope	No	Yes	Yes	Yes
Range of Motion	80° (Yaw)	80° (Yaw)	0°(No articulation)	80° (Yaw)
Sterilization	Difficult	Difficult	Difficult	N/A (disposable)
Instrument Cost	$500-1000	$500-1000	$500-1000	$10-20

Table 7.2. Nerve retractor performance.

Objective	Results	
Articulation at tip of retractor	Articulated tip design	✓
Actuation Range: 80_o	Actuation Range:90-100$_o$	✓
Retraction force up to 0.35 N	Retraction force: 0.54 N	✓

Table 7.3. Grasper performance.

Objective	Results	
Grasper with articulation	No articulation in current design*	~✓
Jaw angle: $30 - 45_o$	Jaw angle:30$_o$	✓
Grasp force: 0.2 N	Maximum grasp force: 1.23 N	✓

*Can be a design combining nerve retractor and grasper, for which the proof of concept has been proved in this project.

7.2 Contributions

Here, a surgical master-slave system is proposed. It combines the positive aspects of MED and arthroscopic procedures in aspects like incision size and manipulation space utilization. The end-effectors are 3D printed and use elastic joints in place of pin joints. This reduces the complexity of the design and keeps the cost of manufacturing low. Combined with the dexterity the end-effectors can provide, and the feature of coordinated manipulation, this system can greatly aid the surgeon in performing the surgery with better success rates. This leads to reduced hospital stay, reduced chances of infection and quicker recovery.

In this work, the manipulators were also evaluated for their performance, mainly their force requirements. A model to describe the joint kinematics of the 1 DOF joint has also been proposed. This is just a preliminary attempt in the design of this surgical system. Although the objective proposes an articulated end-effector, this

work only talks about the implementation of a single joint mechanism and a fixed tool. But these designs show the potential of a 3D printed surgical manipulator which can be used for minimally invasive surgeries. This system can also be expanded to include other tools required for the surgery. The use of 3D printers allow for the customization of manipulator designs to optimize it for other surgeries.

7.3 Future Work

There are many challenges still left to be overcome in this system. These include sterilization, spacing constraints for the actuators, and the design of an efficient control system that can help the surgeon perform this surgery successfully. For this, firstly, the required forces of the manipulator for lumbar discectomy surgery should be estimated. There is little or no literature on the force requirements of the tools for this particular surgery. Estimating this would help in the complete evaluation of the product and can help optimize the design of the manipulator. Another aspect is the measure of the accuracy of these instruments for the surgery and the comfort of the surgeon using these instruments. For this, tests have to be performed with trained surgeons to optimize the design of the surgical system to provide a competitive alternative to the robotic surgical systems in market today.

There could also be improvements in the manufacturing aspect of the surgical manipulators. One particular aspect is the assembly of the end-effector and routing of the cables. In future, procedures to remove support materials and routing cables can be automated to reduce the handling of these instruments before they are used for surgery. The possibility of exploring the capability of the instruments when scaled up for other types of surgery should also be investigated. Also, these manipulators can be designed to be used in existing robotic surgical robots like the daVinci surgical system.

To conclude, this is a preliminary effort in the development of the surgical system. There is a lot of scope to expand this work and build a system capable of handling a variety of surgeries.

LIST OF REFERENCES

LIST OF REFERENCES

[1] L. Ascari, C. Stefanini, U. Bertocchi, and P. Dario. Robot-assisted endoscopic exploration of the spinal cord. *Proceedings of the Institution of Mechanical Engineers, Part C: Journal of Mechanical Engineering Science*, 224(7):1515–1529, 2010.

[2] R. A. Beasley. Medical Robots: Current Systems and Research Directions. *Journal of Robotics*, 2012:1–14, 2012.

[3] A. Bertelsen, J. Melo, E. Sánchez, and D. Borro. A review of surgical robots for spinal interventions. *The International Journal of Medical Robotics and Computer Assisted Surgery*, 9(4):407–422, Dec. 2013.

[4] J. Bodner, H. Wykypiel, G. Wetscher, and T. Schmid. First experiences with the da Vinci operating robot in thoracic surgery. *European Journal of Cardio-thoracic Surgery*, 25(5):844–851, May 2004.

[5] T. Bonaci, J. Yan, J. Herron, T. Kohno, and H. J. Chizeck. Experimental analysis of denial-of-service attacks on teleoperated robotic systems. In *Proceedings of the ACM/IEEE Sixth International Conference on Cyber-Physical Systems - ICCPS '15*, pages 11–20, New York, New York, USA, 2015. ACM Press.

[6] A. A. F. De Salles, A. A. Gorgulho, M. Selch, J. De Marco, and N. Agazaryan. Radiosurgery from the brain to the spine: 20 years experience. *Acta Neurochirurgica, Supplementum*, (101):163–168, 2008.

[7] DLR. *DLR MICA Surgical Instrument*, (accessed November 9, 2015). `http://www.dlr.de/rmc/rm/en/desktopdefault.aspx/tabid-3829/6255_read-9015/`.

[8] DLR. *DLR MiroSurge Robotic System*, (accessed November 9, 2015). `http://www.dlr.de/rm/en/desktopdefault.aspx/tabid-3835/6288_read-9047/`.

[9] L. S. Gan, K. Zareinia, S. Lama, Y. Maddahi, F. W. Yang, and G. R. Sutherland. Quantification of Forces During a Neurosurgical Procedure: A Pilot Study. *World Neurosurgery*, 84(2):537–548, Aug. 2015.

[10] G. Gupta. *Laminectomy*, (accessed November 20, 2015). `http://www.drgguptaortho.com/spine-liminectomy.php`.

[11] V. Gupta, N. Reddy, and P. Batur. Forces in surgical tools: comparison between laparoscopic and\nsurgical forceps. *Proceedings of 18th Annual International Conference of the IEEE Engineering in Medicine and Biology Society*, 1(2):223–224, 1996.

[12] F. U. Hermantin, T. Peters, L. Quartararo, and P. Kambin. A prospective, randomized study comparing the results of open discectomy with those of video-assisted arthroscopic microdiscectomy. *The Journal of bone and joint surgery. American volume*, 81(7):958–965, 1999.

[13] L. L. Howell. *Compliant Mechanisms*. John Wiley & Sons, 2001.

[14] T. S. Innovations. *Phantom MC Nerve Root Retractor*, (accessed November 20, 2015). `http://www.tedansurgical.com/phantom-mc-nerve-root-retractor-p-480.html`.

[15] L. Instruments. *Full Curved Dissector*, (accessed November 20, 2015). `http://www.lifeinstruments.com/450_SPElevator.htm`.

[16] L. Instruments. *Toothed Pituitary IVD Rongeurs*, (accessed November 20, 2015). `http://www.lifeinstruments.com/63_SPRongeur.htm`.

[17] I. Intuitive Surgical. *Intuitive Surgical Needle Drivers*, (accessed November 14, 2015). `http://www.intuitivesurgical.com/products/instruments/`.

[18] I. Intuitive Surgical. *Intuitive Surgical Si System: Overview of Firefly Fluorescence Imaging*, (accessed November 14, 2015). `http://intuitivesurgical.com/company/media/images/firefly.html`.

[19] F. Jelínek, R. Pessers, and P. Breedveld. DragonFlex Smart Steerable Laparoscopic Instrument. *Journal of Medical Devices*, 8(1):015001, Jan. 2014.

[20] P. Kambin. Arthroscopic microdiscectomy. *The Spine Journal*, 3(3):60–64, 2003.

[21] M. Ltd. *micro ScoutCam LEDprobe 1.8mm Diameter Camera*, (accessed November 20, 2015). `http://www.microscoutcam.com/products-and-technology/ledprobe`.

[22] M. Matsumoto, K. Ishii, K. Watanabe, T. Tsuji, M. Nakamura, Y. Toyama, and K. Chiba. Microendoscopic discectomy for recurrent lumbar disc herniation*. *Asian Journal of Endoscopic Surgery*, 3(2):77–82, 2010.

[23] medGadget. *Renaissance spinal robotic surgical guidance system*, (accessed November 20, 2015). `http://www.medgadget.com/2011/06/mazors-new-renaissance-robotic-spinal-surgery-system.html`.

[24] N. T. Nguyen, H. S. Ho, W. D. Smith, C. Philipps, C. Lewis, R. M. De Vera, and R. Berguer. An ergonomic evaluation of surgeons axial skeletal and upper extremity movements during laparoscopic and open surgery. *The American Journal of Surgery*, 182(6):720–724, Dec. 2001.

[25] E. Oberg, F. D. Jones, H. L. Horton, and H. H. Ryffel. *Machinery's Handbook (28th Edition) & Guide to Machinery's Handbook*. Industrial Press, 2008.

[26] M. J. Perez-Cruet, K. T. Foley, R. E. Isaacs, L. Rice-Wyllie, R. Wellington, M. M. Smith, and R. G. Fessler. Microendoscopic lumbar discectomy: Technical note. *Neurosurgery*, 51(November):129–136, 2002.

[27] PhysioWorks. *Bulging Disc*, (accessed November 20, 2015). `http://physioworks.com.au/injuries-conditions-1/bulging_disc`.

[28] Pololu. *Stepper Motor with 18cm Lead Screw*, (accessed November 20, 2015). `https://www.pololu.com/product/2689`.

[29] K. Ponnusamy, S. Chewning, and C. Mohr. Robotic approaches to the posterior spine. *Spine*, 34(19):2104–2109, 2009.

[30] T. M. Rankin, N. A. Giovinco, D. J. Cucher, G. Watts, B. Hurwitz, and D. G. Armstrong. Three-dimensional printing surgical instruments: are we there yet? *Journal of Surgical Research*, 189(2):193–197, 2014.

[31] O. Righesso, A. Falavigna, and O. Avanzi. Comparison of Open Discectomy With Microendoscopic Discectomy in Lumbar Disc Herniations:Results of a Randomized Controlled Trial. *Neurosurgery*, 61(3):545–549, 2007.

[32] K. Shah and R. Abaza. Comparison of intraoperative outcomes using the new and old generation da Vinci robot for robot-assisted laparoscopic prostatectomy. *BJU International*, 108(10):1642–1645, 2011.

[33] S. N. Shaikh. Natural orifice translumenal surgery: Flexible platform review. *World Journal of Gastrointestinal Surgery*, 2(6):210, 2010.

[34] H. Takahashi, S. Warisawa, M. Mitsuishi, J. Arata, and M. Hashizume. Development of High Dexterity Minimally Invasive Surgical System with Augmented Force Feedback Capability. In *The First IEEE/RAS-EMBS International Conference on Biomedical Robotics and Biomechatronics, 2006. BioRob 2006.*, pages 284–289. IEEE.

[35] K. Takahashi, I. Shima, and R. W. Porter. Nerve root pressure in lumbar disc herniation. *Spine*, 24(19):2003–6, 1999.

[36] R. H. Taylor and D. Stoianovici. Medical Robotics in Computer-Integrated Surgery, 2003.

[37] G. Tholey, A. Pillarisetti, W. Green, J. P. Desai, and I. Sensing. Direct 3-D Force Measurement Capability in an Auto- 1 mated Laparoscopic Grasper. *Proceedings of the Eurohaptics 2004 conference*, (1):478–481, 2004.

[38] G. Tortora, P. Dario, and A. Menciassi. Array of robots augmenting the kinematics of endocavitary surgery. *IEEE/ASME Transactions on Mechatronics*, 19(6):1821–1829, 2014.

[39] Trossenrobotics. *Arbotix-M Microcontroller*, (accessed November 14, 2015). `http://www.trossenrobotics.com/p/arbotix-robot-controller.aspx`.

[40] D. E. Vogtmann, S. K. Gupta, and S. Bergbreiter. Characterization and Modeling of Elastomeric Joints in Miniature Compliant Mechanisms. *Journal of Mechanisms and Robotics*, 5(4):041017, 2013.

[41] R. J. Webster and B. A. Jones. Design and Kinematic Modeling of Constant Curvature Continuum Robots: A Review. *The International Journal of Robotics Research*, 29(13):1661–1683, 2010.

[42] M. William O. Reed, Jr. *Arthroscopic Microdiscectomy*, (accessed November 20, 2015). `http://www.handandspine.com/forms/AMDbrochure.pdf`.

[43] H. Yamashita, K. Matsumiya, K. Masamune, H. Liao, T. Chiba, and T. Dohi. Two-DOFs bending forceps manipulator of 3.5-mm diameter for intrauterine fetus surgery: Feasibility evaluation. *International Journal of Computer Assisted Radiology and Surgery*, 1(SUPPL. 1):218–220, 2006.

[44] H. Yamashita, K. Matsumiya, K. Masamune, H. Liao, T. Chiba, and T. Dohi. Two-DOFs bending forceps manipulator of 3.5-mm diameter for intrauterine fetus surgery: Feasibility evaluation. *International Journal of Computer Assisted Radiology and Surgery*, 1(SUPPL. 1):218–220, 2006.

[45] B. P. M. Yeung and T. Gourlay. A technical review of flexible endoscopic multitasking platforms. *International Journal of Surgery*, 10(7):345–354, 2012.